Design of Selective and Soluble Inhibitors of Tumor Necrosis Factor-α Converting Enzyme (TACE)[+]

Michael H. Rabinowitz,*[,†] Robert C. Andrews,[†,⊥] J. David Becherer,[‡] D. Mark Bickett,[‡] Dulce G. Bubacz,[†] James G. Conway,[§] David J. Cowan,[†] Micheal Gaul,[†,&] Kimberly Glennon,[†] Millard H. Lambert,[†] M. Anthony Leesnitzer,[‡] Darryl L. McDougald,[†] Marcia L. Moss,[‡,#] David L. Musso,[†] and Michele C. Rizzolio[||]

GlaxoSmithKline, Five Moore Drive, Research Triangle Park, North Carolina 27709

Received June 13, 2001

A program to improve upon the in vitro, in vivo, and physicochemical properties of *N*-hydroxyformamide TACE inhibitor GW 3333 (**1**) is described. Using the primary structure of pro-TNF-α, along with a homology model of the catalytic domain of TACE based on the X-ray diffraction coordinates of adamalysin, we synthesized *N*-hydroxyformamide TACE inhibitors containing a P2′ arginine side chain. Introduction of nitro and sulfonyl electron-withdrawing groups covalently bound to the P2′ guanidine moiety rendered the inhibitors electronically neutral at cellular pH and led to potent inhibition of TNF-α release from stimulated macrophages. Inhibitors containing these arginine mimetics were found to have increased solubility in simulated gastric fluid (SGF) relative to **1**, allowing for the incorporation of lipophilic P1′ side chains which had the effect of retaining potent TACE inhibition, but reducing potency against matrix metalloproteases (MMPs) thus increasing overall selectivity against MMP1, MMP3, and MMP9. Selected compounds showed good to excellent in vivo TNF inhibition when administered via subcutaneous injection. One inhibitor, **28a**, with roughly 10× selectivity over MMP1 and MMP3 and high solubility in SGF, was evaluated in the rat zymosan-induced pleuisy model of inflammation and found to inhibit zymosan-stimulated pleural TNF-α elevation by 30%.

Introduction

Tumor necrosis factor-α (TNF-α) is a potent proinflammatory cytokine that is produced by many different cell types, including lymphocytes, mast cells, and polymorphonuclear cells, but primarily by activated monocytes and macrophages.[1,2] Overproduction of TNF-α is strongly correlated with diverse pathologies such as HIV infection,[3] rheumatoid arthritis,[4] septic shock,[5] insulin resistance,[6] and graft rejection.[7] TNF-α is produced as a 233 amino acid, 26 kDa membrane-bound pro form which is found in the plasma membrane as well as localized in intracellular compartments. It is processed to a soluble 17 kDa form by proteolysis at Ala[76]-Val[77] by tumor necrosis factor-α converting enzyme (TACE), a membrane-bound zinc metalloprotease.[8,9] Both the 26 kDa pro form and the 17 kDa mature form are active only as trimers which are thought to induce signaling by trimerizing the TNF receptor upon binding.[10,11]

Two TNF-α receptors are known: the 55 kDa TNFR1 which is thought to be present on all cell types, and the 75 kDa TNFR2 found predominantly on endothelial and blood cells. It is signaling through the p55 receptor that is thought to be responsible for most of the pro-inflammatory effects of TNF-α.[12] Both membrane-bound and soluble forms of each receptor have been found,[13] and are believed to play important roles in immunoregulation in nonpathological states. Binding of the TNF-α trimer to TNFR leads to the induction of apoptosis through tyrosine kinase signaling which activates transcription factors such as NF-κB.[14]

A number of therapeutic strategies have been proposed for inhibition of the pro-inflammatory TNF-α signaling pathway. In addition to soluble receptor therapy, inhibition of protein phosphorylation with kinase inhibitors[14] and antisense treatment[15,16] have been shown to inhibit the activation of NF-κB by TNF-α. A monoclonal humanized mouse anti-TNF antibody (Remicade) is currently marketed for the treatment of rheumatoid arthritis and Crohn's Disease.[17] A dimeric fusion protein of the soluble p75 receptor and human IgG1 is currently sold as Enbrel and has proven effective in treating rheumatoid arthritis.[18] A drawback of both the monoclonal antibody and soluble receptor therapies is the possibility of serious infections and sepsis resulting from complete inhibition of TNF-α signaling.[19] Also potentially problematic is the development of autoantibodies in patients receiving these therapies.[20,21] Another approach has been the development of TNFR1 antagonists via modeling of the TNF receptor−ligand complex.[22] A final strategy for the intervention of TNF-promoted inflammation is inhibition of the biosynthesis of TNF-α either via prevention of its production at the transcriptional level or by inhibition of its posttranslational processing. Inhibitors of p38 MAP kinase act via inhibiting the gene expression of a number of cytokines

[+] A preliminary account of this work was presented at the 220th meeting of the American Chemical Society, August 20−21, 2000, Washington, D.C.

* Address correspondence to current address: R. W. Johnson Pharmaceutical Research Institute, 3210 Merryfield Row, San Diego, CA 92121. Tel: (858) 320-3340. Fax: (858) 784-3267. E-mail: mrabinow@prius.jnj.com.

[†] Division of Chemistry.

[‡] Division of Molecular Biochemistry.

[§] Department of Molecular Pharmacology.

[||] Department of Pharmaceutical Development.

[⊥] Current Address: TransTech Pharma Inc., 4170 Mendenhall Oaks Parkway, Suite 110, High Point, NC 27265.

[#] Current Address: Cognosci, Inc., 2 Davis Dr., P. O. Box 12076, Research Triangle Park, NC 27709.

[&] Current Address: 3-Dimensional Pharmaceuticals, Inc., 665 Stockton Drive, Suite 104, Exton, PA 19341-1151.

10.1021/jm0102654 CCC: $20.00
Published on Web 10/16/2001

including TNF.[23] The approach that we have chosen is inhibition of the processing of 26 kDa via inhibition of TACE, which is expected to reduce levels of soluble 17 kDa TNF-α while not interfering with the production or function of the 26 kDa cell-associated form.

The suggestion that TACE is a metalloprotease was first proposed in 1994[24,25,26] when it was discovered that small molecule metalloprotease inhibitors could inhibit soluble TNF-α production in stimulated macrophages with little effect on the production of other cytokines. Subsequently in 1997, TACE was isolated, purified, cloned, and characterized.[27,28] In addition to a Zn-binding HExxHxxGxxH motif, TACE was found to contain a signal peptide domain, a "cysteine-switch" pro-domain, a disintegrin domain, a cysteine-rich domain, a transmembrane segment, and a cytosolic tail[29] making it a member of the ADAM/reprolysin family of metalloproteases. Its primary sequence is most closely related to that of the metalloprotease ADAM-10.[9] TACE is found to a small degree on the cell surface but is considered to exist predominantly in the perinuclear space, and it is hypothesized that the action of TACE on the ectodomain shedding of TNF-α may occur largely in an intracellular compartment.[30] Indeed, we have observed a lack of correlation between small molecule TACE inhibitors in the enzyme and whole-cell TNF release assays supporting the idea that therapeutically useful small molecule TACE inhibitors not only have to be potent inhibitors of the free enzyme, but also must have the appropriate physicochemical properties to allow cell penetration.[31]

The goals of our inhibitor program were to create a soluble, orally bioavailable small molecule inhibitor of TACE. In addition, because of reports of tendonitic adverse effects leading to joint pain in humans treated with nonselective MMP inhibitors,[32,33] we desired good selectivity for TACE over MMPs such as collagenase 1 (MMP1), gelatinase B (MMP9), and stromelysin 1 (MMP3). We have developed a number of potent small molecule *N*-hydroxyformamide inhibitors with either 2-pyridyl or 2-thiazolyl amides occupying the P3′ positions, of which **1** is representative. Compound **1** is a potent inhibitor of TACE that has been shown to completely inhibit LPS-induced TNF-α production in mice after oral administration.[31] It has also been shown to be effective in the peptidoglycan polysaccharide (PGPS) reactivation arthritis model in the rat.[34,35] However, this compound is not selective for TACE versus other MMPs leading to the possibility of tendonitic side effects in vivo. Additionally, **1** was found to have a solubility in simulated gastric fluid (SGF) of 0.08 mg/mL making formulation and further compound development potentially problematic. In this article, we disclose our efforts toward identifying TACE inhibitors with improved aqueous solubility and metalloprotease selectivity.

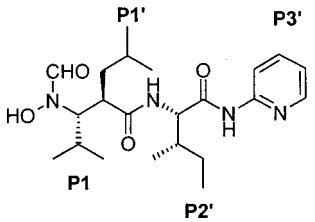

GW 3333 (1)

Inhibitor Design

Discoveries made in our laboratories have already shown that good selectivity for TACE over MMPs could be obtained with large lipophilic substituents at either the P1 or P1′ positions of *N*-hydroxyformamide inhibitors.[36] Unfortunately, these substitutions had the effect of further decreasing the already low aqueous solubility of this class of TACE inhibitor. We reasoned that by incorporating the P2′ arginine (Arg) residue of 26 kDa TNF-α into our small molecule inhibitors we could increase the solubility of the inhibitors such as to allow the incorporation of lipophilic groups at P1 and P1′. Because of the expectation that the charged guanidinium side chain of arginine would render inhibitor molecules unable to reach the intracellular enzyme (vide supra), we turned our attention to a homology model[37] of TACE that was created by modeling the primary sequence of the catalytic domain of TACE onto the known X-ray structure of the snake venom metalloprotease adamalysin[38] using the MVP program.[39] (Indeed, cationic *N*-hydroxyformamide P2′ Arg inhibitors synthesized in parallel format displayed low nM inhibition of TACE in the enzyme SPA assay but failed to inhibit TNF-α release in LPS stimulated Monomac 6 cells even at the highest doses tested (unpublished results).) Various *N*-hydroxyformamide inhibitors were docked into the model using MVP. Docking calculations with arginine at the P2′ position suggested that the arginine side chain would extend generally outward from the enzyme active site cleft. Several side chain conformations are possible, including conformations where the guanidinium group makes hydrogen bonds with the backbone carbonyl of Met345 or with the side-chain hydroxyl of Thr347. Similar interactions with the arginine at the same position in the 26 kDa TNFα substrate could account for some of the enzyme's substrate selectivity.

These interactions would depend primarily on the hydrogen bonding character of the guanidinium group, rather than its net electrical charge. The model suggested that, even when an inhibitor makes these hydrogen bonding interactions, there would still be adequate space available around the guanidinium group for further functional group substitution. This supported our belief that small electron-withdrawing groups attached to the guanidinium array of the P2′ residue of the inhibitors would be sterically tolerated. More importantly, addition of such an electron-withdrawing group would reduce the basicity of the guanidine, rendering it electronically neutral at physiological pH.[40] After this analysis, the X-ray structure of the catalytic domain of TACE was published,[41] supporting the assumptions made using our homology model. The docking of a P2′-nitroguanidinium inhibitor into the crystallographic structure of TACE is shown in Figure 1.

Targets chosen to evaluate this hypothesis were *N*-hydroxyformamide inhibitors containing nitro-Arg, methanesulfonyl-Arg, and 2-pyridylsulfonyl-Arg occupying the P2′ position. Additionally, in hopes of stabilizing the central amide bond in analogy to P2′ branched side chains similar to those found in orally bioavailable inhibitors such as **1** and marimastat, we sought inhibitors containing P2′ *β*-methyl and *β*,*β*-dimethyl substituted Arg (e.g., **2** and **3**, EWG = electron withdrawing group).

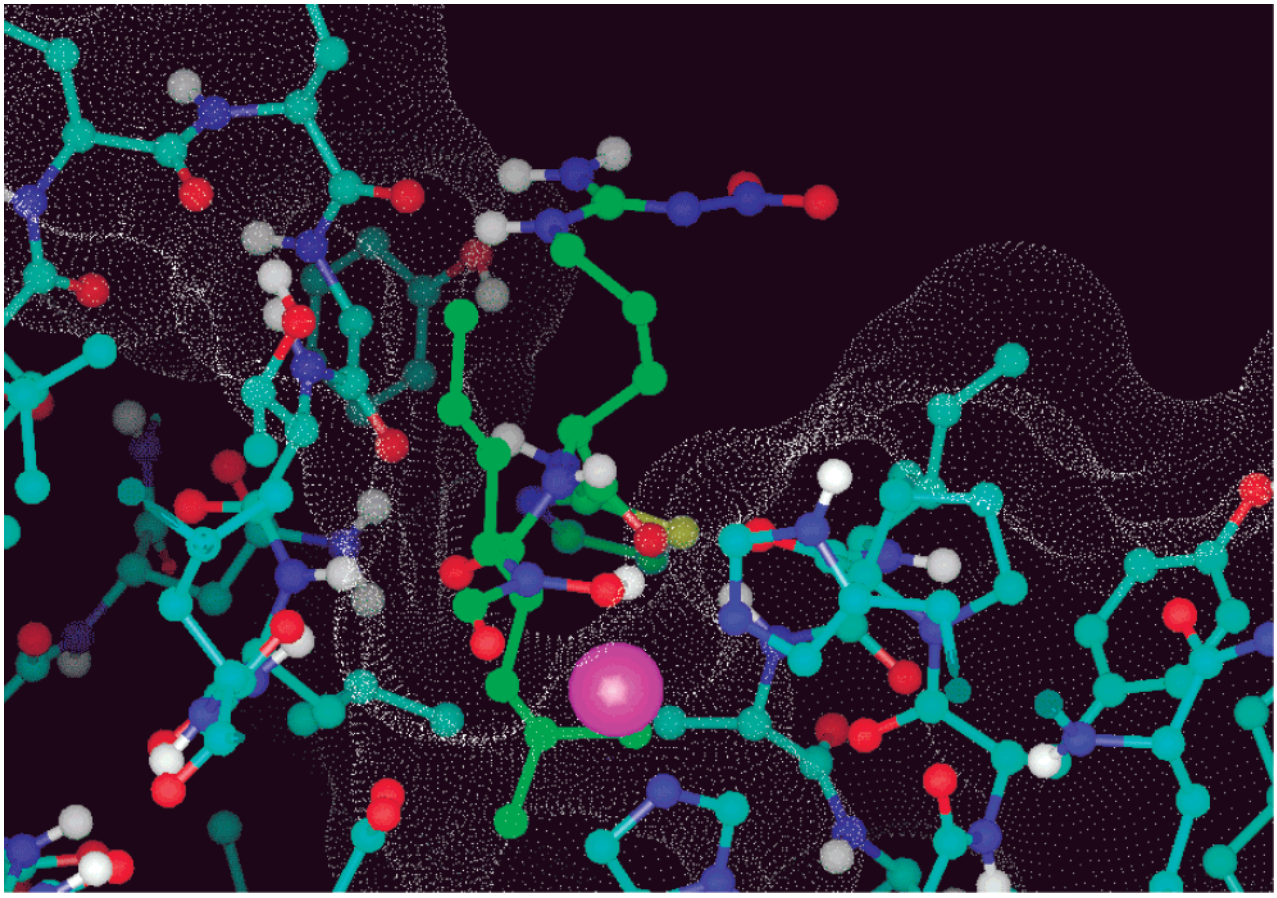

Figure 1. Compound **28a** docked in the active site binding pocket of the X-ray structure of the TACE catalytic domain.[41] The nitroarginine-containing P2′ side chain can be seen extending into solvent space. Compound **28a** was docked and minimized using the MVP program.[39] Hydrogen, nitrogen, oxygen, sulfur, and zinc atoms are shown in white, blue, red, yellow, and purple, respectively. Carbon atoms are blue and green in the protein and inhibitor, respectively. The surface of the protein is depicted with a Connolly dot surface.

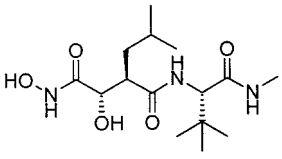

Marimastat

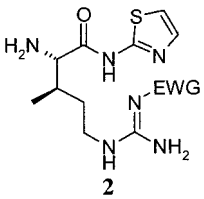

2

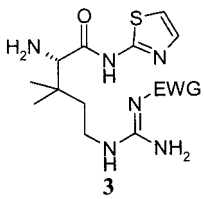

3

Biology

Metalloprotease inhibitors **28a**−**u** were evaluated in vitro to determine their inhibition potency against matrix metalloproteases MMP1, MMP3, and MMP9 using a fluorescence-based peptide assay.[42]

The inhibition of TACE was measured with a scintillation proximity assay (SPA) peptide construct as described previously.[43]

Compounds that displayed significant potency in the SPA assay were subsequently evaluated in a whole-cell assay to determine their potency of inhibition of TNF-α release by the action of TACE under more physiologically relevant conditions. Thus, human Mono Mac-6 mononuclear cells were preincubated with inhibitor and then stimulated with LPS. Soluble TNF-α released in the media was quantified via ELISA assay.[26,44]

Compounds with sufficient potency in the whole-cell TNF-α release assay were then evaluated for their in vivo activity following an inflammatory challenge. TACE inhibitor was administered by subcutaneous (sc) injection or oral gavage (40 mg/kg) to female mice 10 min prior to intraperitoneal (ip) injection of lipopolysaccharide (LPS, 0.2 mg/kg). Plasma levels of TNF-α were measured at 90 min post LPS injection and quantified using an ELISA assay.

A zymosan-induced rat pleurisy was used to evaluate compounds in a model of inflammation. Intrapleural injection of zymosan produced an inflammatory response in the pleural cavity signified by neutrophil infiltration and elevated cytokine levels. TNF-α titers in the pleural exudate were quantified by ELISA assay after pretreatment with either vehicle or TACE inhibitor.[35]

Scheme 1[a]

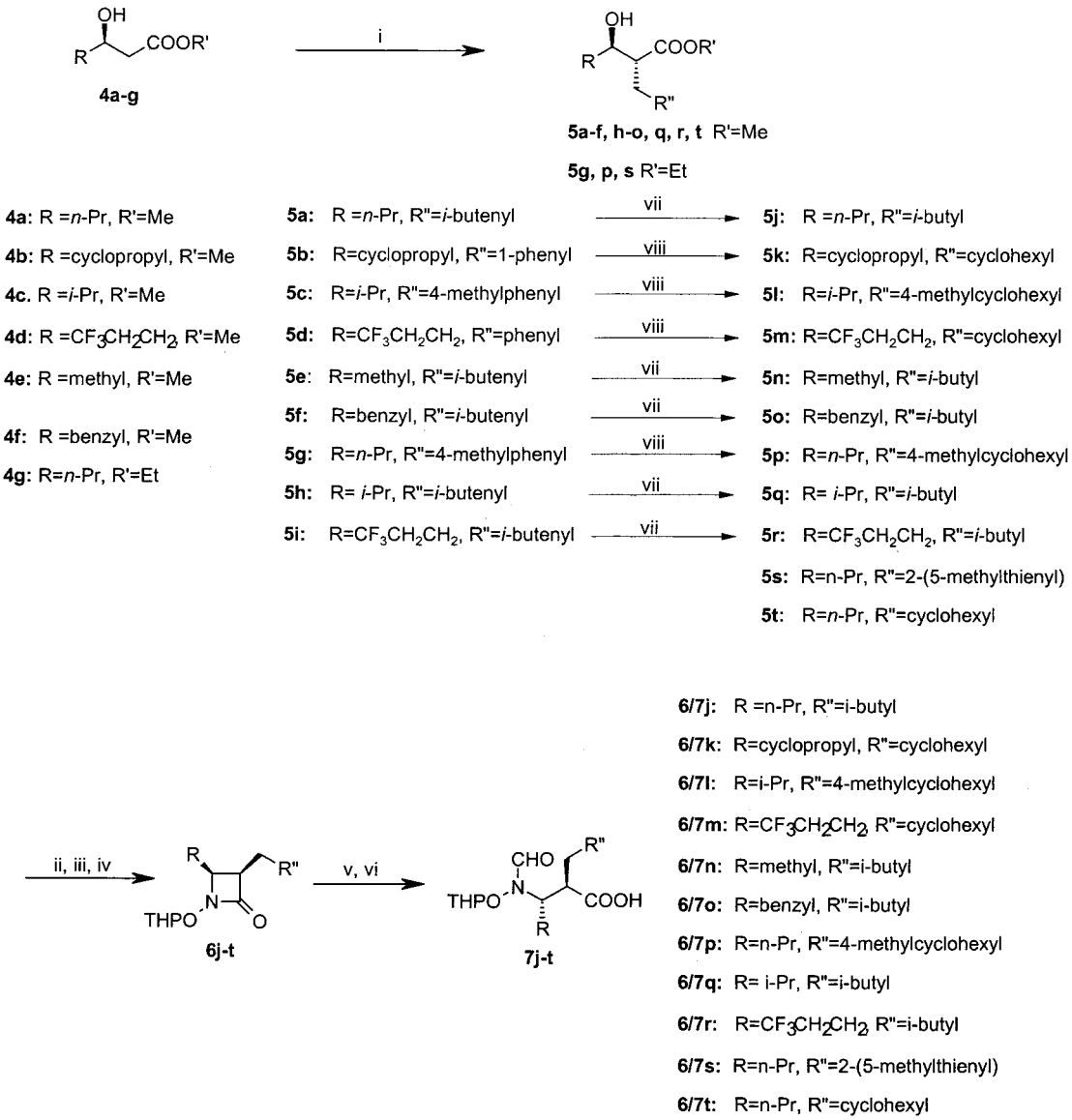

[a] Reagents: (i) LDA, alkyl halide, THF, DMPU, −78 °C to 0 °C, 12−48 h; (ii) LiOH, THF, MeOH, H_2O, 12 h; (iii) $THPONH_2$, DCC, EtOAc, 0 °C to RT, 3−6 h; (iv) *a*. MsCl, pyridine, 0 °C, 6 −12 h; *b*. Me_2CO, K_2CO_3, reflux, 12 h; (v) NaOH, dioxane, H_2O, RT, 24 h; (vi) AcOCHO, pyridine, DCM, 0 °C, 1 h; (vii) H_2 Pd/C or $Pd(OH)_2$, MeOH, 3−13 h; (viii) H_2, Rh/Al_2O_3, MeOH, 70 psi, 24−48 h.

Chemistry

Synthesis of the P1−P1′ left-hand portions of the *N*-hydroxyformamide inhibitors was carried out as depicted in Scheme 1. Enantioenriched (*R*)-*β*-hydroxyesters **4a**−**g** were prepared by Noyori asymmetric reduction of the corresponding *β*-ketoesters.[45] Frater-Seebach alkylation[46] of the lithium enolates of **4a**−**g** with an appropriate alkyl, allylic, or benzylic halide resulted in anti aldols **5a**−**i**, **5s**, and **5t**. Diastereoselectivity of 10:1 to 15:1 was typically observed, with the minor syn diastereomer being removed by silica gel chromatography either at this stage, or at the azetidinone stage. Hydrogenation of olefinic aldol products (H_2, Pd) and the benzylic aldol products (H_2, Rh) resulted in fully saturated esters **5j**−**r**. Ester hydrolysis (aqueous LiOH), hydroxamate formation ($THPONH_2$, DCC), and cyclization (MsCl, pyridine then K_2CO_3) gave rise to the corresponding (*3R, 4S*) azetidinones **6j**−**t**. The completed left-hand acid coupling partners were then prepared from **6j**−**t** through *β*-lactam hydrolysis with NaOH in aqueous dioxane followed by formylation with freshly prepared acetic formic anhydride in pyridine.[47] Acids **7j**−**t** could then be used either in their crude forms or purified on silica gel as their pentafluorophenyl esters (prepared by esterification with pentafluorophenol and DCC).

N^G-Substituted arginine analogues **9**, **11**, and **15** were synthesized as shown in Scheme 2. Coupling of commercially available Nα-Boc-N^G-nitroArg (**8**) with 2-aminothiazole followed by Boc removal afforded P2′-P3′ right-hand piece **9**. Sulfonylation of Nα-Boc Arg (**10**) with 2-chlorosulfonylpyridine[48] in water followed by coupling with 2-aminothiazole and Boc deprotection provided P2′ N^G-2-pyridylsulfonyl coupling partner **11**. Synthesis of N^G-methanesulfonyl Arg derivative **15** could not be achieved by sulfonylation with methanesulfonyl chloride owing to this reagent's instability in water. An indirect route involved the construction of the mesylguanidine moiety by treatment of Nα-Boc ornithine (**12**) with dimethyl methylsulfonyldithioimidocar-

Scheme 2[a]

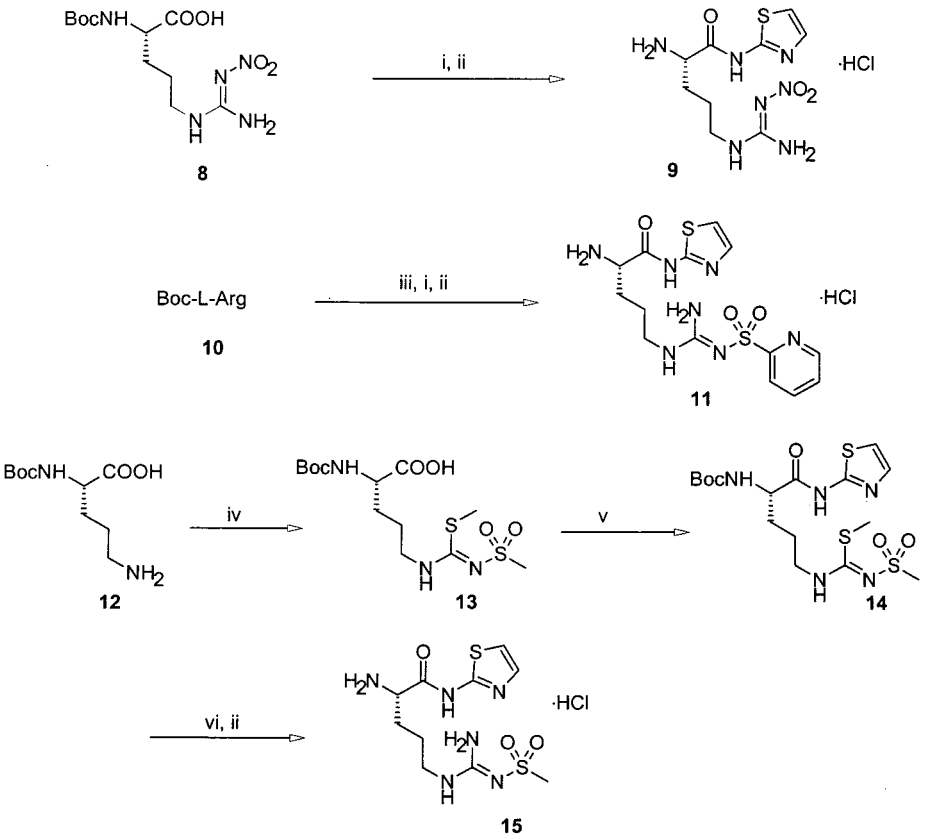

[a] Reagents: (i) 2-Aminothiazole, EDC, DMF, 25−40 °C, 24−48 h; (ii) HCl, dioxane, 25 °C, 0.3−1 h; (iii) 2-pyridylsulfonyl chloride, NaOH, acetone, H_2O, 0 °C, 5 h; (iv) $MsN{=}C(SMe)_2$, NaOH, EtOH, H_2O, 65 °C then reflux, 15 h; (v) i-BuOCOCl, TEA, DMF, −23 °C, 0.75 h., then 2-aminothiazole, −23 °C to RT; (vi) NH_3 $AgNO_3$, MeCN, 0 to 25 °C, 2 h.

bonate to afford *N*-methanesulfonylisothiourea **13**. Coupling with 2-aminothiazole via the mixed anhydride, guanidine formation (NH_3, $AgNO_3$), and Boc deprotection resulted in the desired methanesulfonylguanidine amino amide **15**.

Attention was then turned toward the synthesis of β-methyl and β,β-gem-dimethyl arginine right-hand pieces.

Amino acid **16a**[49] (85% ee, 9:1 mixture of diastereomers) was converted to Cbz-protected *tert*-butyl ester **17** (Scheme 3) by the sequential treatment with aqueous NaOH, then CbzCl, followed by esterification with dimethylformamide di *tert*-butyl acetal. Hydroboration of alkene **17** with in situ generated thexylborane followed by H_2O_2 oxidation provided primary alcohol **18** in 88% isolated yield with no evidence of regioisomeric 2° alcohol formation. Mesylation and azide formation provided **19** without pyrrolidine formation (as was observed in the attempted synthesis of the β,β-dimethyl Arg analogue (vide infra). Azide reduction via hydrogenation over Lindlar catalyst resulted in amine **20** which could be converted to *N*-mesyl isothiourea **21** through the action of dimethyl methylsulfonyldithioimidocarbonate (71% two steps) or guanidinium salt **24** by treatment with 3,5-dimethylpyrazole-1-carboxamidine nitrate (72%; Scheme 4). Transformation of **21** to Cbz protected right-hand coupling fragment **22** was completed as described for **15** (vide supra).

An attempt to prepare the β,β-dimethyl Arg analogue of **23** (cf. **3**) using a similar sequence, starting with the known β,β-dimethyl amino acid **16b**[50] was hampered by facile cyclization in both the mesylation and azide reduction steps, promoted by the *gem*-dimethyl effect.[51] (See Supporting Information).

The β-methyl arginine derivative **24** (Scheme 4) was transformed to N^G-nitro-Nα-Boc arginine (**25**) via the following four-step sequence: (1) Cbz deprotection (Pd/C, cyclohexadiene); (2) ester cleavage (TFA); (3) nitration (fuming HNO_3, fuming H_2SO_4); and (4) amine protection (Boc_2O, $NaHCO_3$). Amide bond formation with 2-aminothiazole and Boc deprotection as before provided the desired β-methylnitroarginine right-hand piece (**27**).

The desired *N*-hydroxyformamide inhibitors **28a**−**u** were prepared by DEPC mediated amide coupling of THP-protected acids **7j**−**t** with amino amides **9**, **11**, **15**, **23**, and **27** in DMF (Scheme 5). Alternatively, the coupling could be achieved via pentafluorophenyl ester activation of the carboxylic acid. The crude coupled products were purified by silica gel chromatography. In the case of compounds **28q**, **28t**, and **28u**, the minor diastereomers produced from the coupling of stereochemically impure **23** and **27** could be removed at this stage by chromatography. Compounds **28p**, **28r**, and **28s** were evaluated as 85:15 to 90:10 mixtures of diastereomers. Final compounds were then obtained by removal of the THP protecting group with 80% AcOH at 40 °C and purified by trituration to provide TACE inhibitors **28a**−**u** as broad-melting amorphous solids.

Results and Discussion

Inhibitors containing a P2′ nitroarginine side chain (**28a**−**f**, **k**, **l**) showed excellent inhibition of TACE in our

Scheme 3[a]

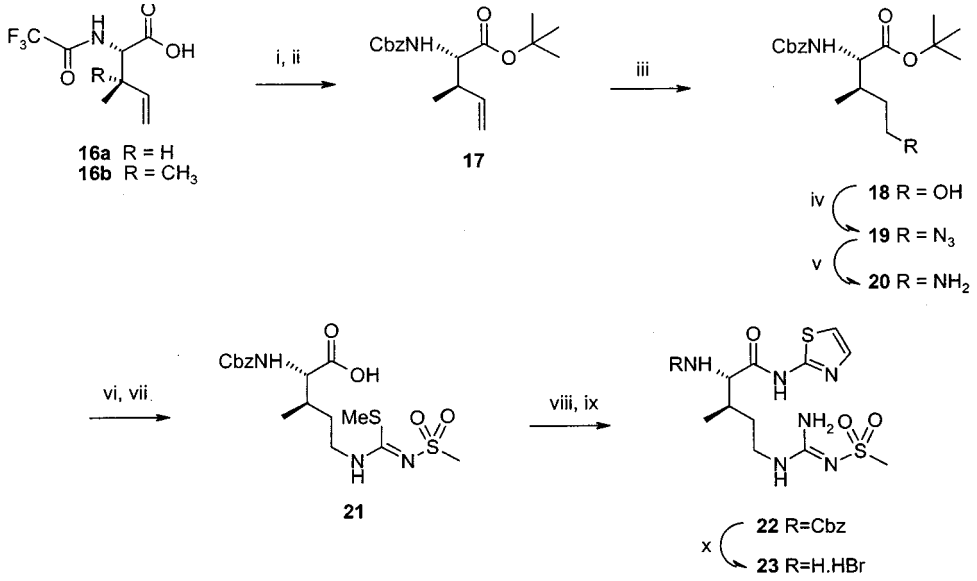

[a] Reagents: (i) NaOH, H_2O, 80 °C, 1 h, then CbzCl, 0 to 23 °C, 30 min; (ii) $(t\text{-BuO})_2CHNMe_2$, toluene, 80 °C, 1 h; (iii) thexylborane, THF, 0 °C, 1 h, then H_2O_2, pH 7.0; (iv) *a*. MsCl, pyridine, DCM, 0 °C, 12 h; *b*. NaN_3, DMF, 40 °C, 12 h; (v) H_2, Lindlar catalyst, TEA, MeOH, 1 h; (vi) $(MeS)_2C{=}NMs$, NaOAc, EtOH, H_2O, reflux; (vii) TFA, thioanisole, H_2O, DCM (88:5:5:2), 23 °C, 60 min; (viii) *a*. *i*-BuOCOCl, NMM, DMF, −23 °C, 0.5 h; *b*. 2-aminothiazole, −23 °C to RT, 14 h; (ix) NH_3, $AgNO_3$, MeOH, 0 to 23 °C, 2 h; (x) HBr, AcOH, 23 °C, 0.5 h.

Scheme 4[a]

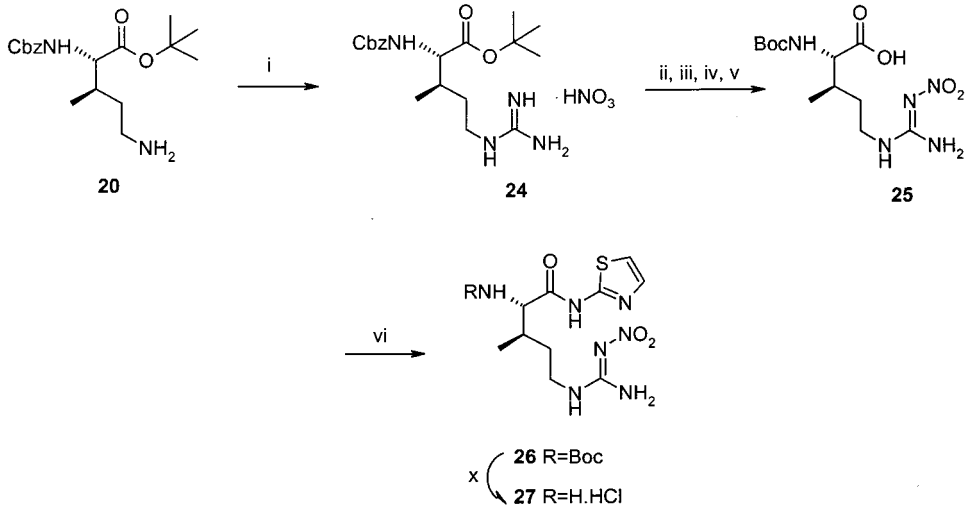

[a] Reagents: (i) 3,5-Dimethylpyrazole-1-carboxamidine nitrate, TEA, DMF, 23 °C, 72 h; (ii) 10% Pd/C, 1,4-cyclohexadiene, MeOH, reflux, 60 min; (iii) TFA, H_2O, 6 h; (iv) fuming HNO_3, fuming H_2SO_4; (v) di-*t*-butyldicarbonate, $NaHCO_3$, H_2O, THF, RT, 18 h; (vi) *i*-BuOCOCl, TEA, DMF, −15 °C, then 2-aminothiazole, −15 to 23 °C, 18 h; (x) HCl, dioxane, 23 °C, 2 h.

SPA assay (IC_{50} = 4.3−49 nM; Table 1). Variation of the P1 substituent between straight chain and branched aliphatic groups had little effect on enzyme potency. However, the placement of a benzyl group at this position reduced affinity for TACE by ca. 10-fold (cf. **28a** and **28l**). These results are consistent with the expectation that the P1 substituent, like the P2′ substituent, projects out from the enzyme active site into surrounding solvent, permitting moderate steric bulk at this position. With respect to TACE inhibition, substitution at the P1′ position also seems to be tolerant of a variety of alkyl and aromatic groups such as isobutyl (**28a** and **28l**), cyclohexyl (**28b**, **28d**, and **28k**), 4-methylcyclohexyl (**28e** and **f**), and simple aromatic groups (5-methylthien-2-yl, **28c**). Selectivity for TACE over MMP1, MMP9, and MMP3, however, is strongly influenced by the choice of substituent at this position. Comparing **28a**, **28c**, **28d**, and **28f**, where the P1 substituent is held constant (*n*-Pr), selectivities progress from low TACE selectivity over MMPs (**28a**, **28l**, P1′ = isobutyl) to high selectivity against MMP1 (IC_{50} >2500 nM) (**28c**, P1′ = 5-methylthien-2-yl). In the case of the inhibitors shown in Table 1, three compounds, **28b**, **28c**, and **28f**, display greater than 10-fold selectivity against MMP9. These represent some of the most selective TACE inhibitors over MMP9 in the *N*-hydroxy formamide series.

As mentioned above, *N*-hydroxyformamide inhibitors containing the charged guanidinium residue of arginine in the P2′ position fail to inhibit TNF release from LPS-stimulated mononuclear cells. However, as Table 1 shows, the electronically neutral nitroarginine inhibitors show good to excellent inhibition of TNF release from

Scheme 5[a]

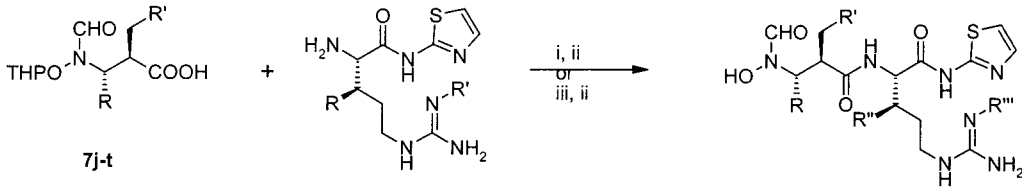

9 R = H, R' = NO_2

11 R = H, R' = 2-pyridylsulfonyl

15 R = H, R' = Ms

23 R = Me, R' = Ms

27 R =Me, R' = NO_2

28a-u*

[a] Reagents: (i) DEPC, NMM, DMF, 12−16 h, 23 °C; (ii) AcOH, H_2O, 40 °C, 16−20 h; (iii) pentafluorophenol, DCC, 0−23 °C, 2h. *See tables 1−3 for the identities of R, R′, R″, and R‴.

Table 1. In Vitro and Solubility Profiles of P2′ Nitro-arginine Inhibitors

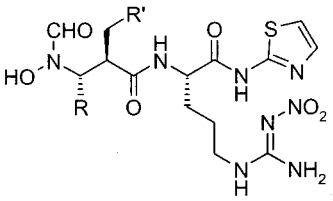

Structure			Enzyme Inhibition[a]				TNF rel.[d]	SGF Sol.[e]
No.	R	R'	TACE[b]	MMP1[c]	MMP9[c]	MMP3[c]		
28a			4.3	34	13	31	34	>1.6
28b			22	144	602	1490	350	0.92
28c		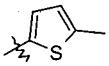	9.0	>2500	190	79	140	ND[f]
28d			8.0	108	55	203	32	0.33
28e		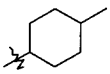	8.0	85	35	76	23	0.21
28f		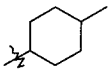	9.0	188	115	200	56	0.16
28k			5	110	49	214	90	0.054
28l	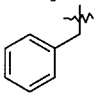		49	26	11	31	420	ND[f]

[a] IC_{50} (nM). Standard errors for enzyme assays were typically ±30% of the mean or less. [b] SPA assay (see text). [c] Fluorescence assay (see text). [d] Inhibition of TNF release from mononuclear cells following LPS stimulation (see text); IC 50 (nM). [e] Solubility in mg/mL in simulated gastric fluid. ">" Indicates full solubility at the highest concentration tested. [f] Not determined.

whole cells (IC_{50} 23−420 nM), presumably due to the neutral arginine mimetic's ability to diffuse or be transported through the plasma membrane.

The solubility of P2′ nitro-arginine inhibitors also displayed, in general, a marked improvement over earlier compounds such as **1**. With the exception of the

Table 2. In Vitro and Solubility Profiles of P2′ Methanesulfonyl-arginine and 2-Pyridylsulfonyl-arginine Inhibitors

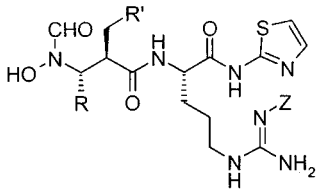

Structure			Enzyme Inhibition[a]				TNF rel.[d]	SGF Sol.[e]
Z = Methanesulfonyl			TACE[b]	MMP1[c]	MMP9[c]	MMP3[c]		
No.	R	R'						
28m			42	21	22	62	252	ND[f]
28n			7.9	100.	51	122	431	>1.13
28o		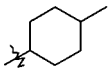	14	122	89	155	400	1.4
Z = 2-Pyridylsulfonyl								
28g		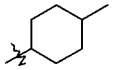	6.0	133	143	282	190	0.16
28h		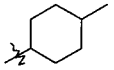	16	96	71	115	120	ND[f]
28i		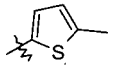	11	>2700	379	218	290	ND[f]
28j			6.0	76	43	84	81	ND[f]

[a] IC_{50} (nM). Standard errors for enzyme assays were typically ±30% of the mean or less. [b] SPA assay (see text). [c] Fluorescence assay (see text). [d] Inhibition of TNF release from mononuclear cells following LPS stimulation (see text); IC_{50} (nM). [e] Solubility in mg/mL in simulated gastric fluid. ">" Indicates full solubility at the highest concentration tested. [f] Not determined.

trifluorinated inhibitor **28k**, all compounds tested showed solubilities in SGF (Table 1) from 2- to over 20-fold greater than that of **1** (0.08 mg/mL, SGF; Table 1). In the case of the TACE inhibitors which are selective over MMP1 (**28b**, **28d**, and **28f**) increased solubility was observed even with lipophilic cyclohexyl and 5-methylcyclohexyl substituents at P2′ (cf. **1**).

Evaluation of P2′ sulfonylated arginine derivatives (Table 2) shows a similar pattern of high activity of TACE inhibition (IC_{50} 6.0−42 nM) and selectivity over MMPs. As with the P2′ nitroarginine inhibitors, cycloalkyl and thienyl substituents at P1′ appear to attenuate the inhibition of MMP1, MMP3, and MMP9. However, in the case of the P2′ methanesulfonyl- and 2-pyridylsulfonylarginine inhibitors, inhibition of TNF-α release from whole cells appears to be roughly 2−20-fold less potent then their nitroarginine analogues. This discrepancy is not accounted for by simply considering the difference in enzyme inhibition potencies, and may be due to a difference in the degree of plasma membrane passive diffusion of the two subtypes of inhibitor.

Solubility in SGF was measured for three of the compounds listed in Table 2, and methanesulfonyl- and 2-pyridylsulfonylarginine inhibitors were found to be 2−14 times more soluble than **1**, with improved selectivity over MMPs (Table 2).

Because the β-methylated arginine inhibitors were prepared as chimeras of **1** and Marimastat in hopes of achieving oral bioavailability in th P2′ Arg series, only P1′ isobutyl inhibitors were initially evaluated. N^G-Nitroarginine and methanesulfonylarginine inhibitors bearing methylation at the β-carbon of the central arginine (**28p**−**u**; Table 3) were evaluated in enzyme and whole cell assays. Methylation of **28n**, **28m**, and **28a** (resulting in compounds **28p**, **28r**, and **28s**, respectively) resulted in no loss of potency for TACE inhibition. Other inhibitors (**28u**, **28q**, and **28t**) also showed excellent inhibition of TACE. For compounds in Table 3, good selectivities over stromelysin-1 (MMP3) were found when P1 was methyl, suggesting a preference of MMP3 for larger alkyl groups at this position in the *N*-hydroxyformamide series. Selectivities for MMP1 and MMP9 were modest, supporting our earlier findings that

Table 3. In Vitro and Solubility Profiles of P2′ β-Methyl Methanesulfonylarginine and Nitroarginine Inhibitors

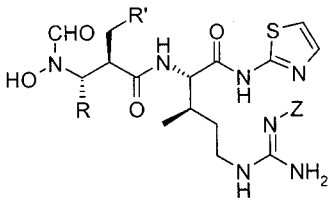

Structure			Enzyme Inhibition[a]				TNF rel.[d]	SGF Sol.[e]
Z = Methanesulfonyl			TACE[b]	MMP1[c]	MMP9[c]	MMP3[c]		
No.	R	R'						
28p			6	57	48	156	25	ND[f]
28u	CH_3		12	18	8.5	169	100	>2.13
28q			8	52	22	17	28	ND[f]
28r			35	8.1	12	49	88	ND[f]
Z = Nitro								
28t	CH_3		7	38	19	273	30	>0.85
28s			5	24	13	47	23	ND[f]

[a] IC50 (nM). Standard errors for enzyme assays were typically ±30% of the mean or less. [b] SPA assay (see text). [c] Fluorescence assay (see text). [d] Inhibition of TNF release from mononuclear cells following LPS stimulation (see text); IC_{50} (nM). [e] Solubility in mg/mL in simulated gastric fluid. ">" Indicates full solubility at the highest concentration tested. [f] Not determined.

TACE selectivity over these enzymes is poor for P1′ isobutyl-containing inhibitors. Although inhibition of TNF-α release for nitroarginine inhibitors **28s** and **28t** was about the same as that for the unmethylated analogues (cf. **28a**), the addition of a β-methyl group to the sulfonylarginine derivatives appears to enhance inhibition potency in the whole-cell assay. Methylated compounds **28p** and **28r** show 17- and 3-fold increased potency over their nonmethylated analogues, **28n** and **28m**, respectively. The solubility in SGF was measured for two of the compounds (**28u** and **28t**) and found to be 10- and over 20-fold greater than that of **1** (Table 3).

In Vivo

Some of the compounds were evaluated for their efficacy in reducing plasma TNF-α levels in mice after stimulation with LPS. Nitroarginine inhibitors **28a**, **28b**, **28d**, **28e**, **28f**, and **28k** were evaluated by both subcutaneous and oral administration at 40 mg/kg body weight. After sc injection, P2′ nitroarginine inhibitors all showed good to excellent inhibition of TNF release in the LPS-treated mouse (Table 4). The most efficacious compound, **28a**, caused near complete inhibition of soluble TNF-α production induced by LPS challenge. These compounds were then evaluated for oral efficacy at 40 mg/kg by oral gavage as a suspension. As Table 4 shows, none of the nitroarginine P2′ inhibitors had any

Table 4. Inhibition of Soluble TNF-α Production in LPS-Stimulated Mice

	%inhibition[a]	
compound	sc[b]	po[c]
28a	96***	−29
28b	56***	−3
28d	72***, 75***	−27, −39*
28e	71***	−6
28f	64***	−19
28h	ND[d]	−9
28j	ND[d]	−28
28k	73***	−24, −34
28o	ND[d]	32
28p	ND[d]	28
28q	ND[d]	−5
28r	ND[d]	7
28s	ND[d]	−10
28t	ND[d]	−2
28u	ND[d]	−3

[a] Percent inhibition of soluble TNF-α as compared to vehicle-treated controls. Vehicle-treated compared to compound using 2-sided *t*-test: *, $P < 0.05$; ***, $P < 0.001$. [b] sc = 40 mg/kg subcutaneous injection 10 minutes prior to ip LPS injection. [c] po = 40 mg/kg oral dose given by gavage 10 minutes prior to ip LPS injection. [d] Not determined.

Table 5. Inhibition of TNF-α Production in Rat Zymosan Inflammation Model

compound	total TNF-α[a]	% inhibition of TNF-α production
vehicle	1442 ± 87.09 (n = 6)	
28a[b]	1004 ± 46.74[c] (n = 6)	30.%

[a] Results are pg in pleural exudate as assayed by ELISA (see text for details). [b] Compound (50 mg/kg) administered sc in aqueous 5% EtOH, 5% propylene glycol, 10% Cremephore, 10% Molecusol suspension (5 mL/kg body weight). [c] $P < 0.01$ (compared with vehicle control using unpaired two-sided t-test).

effect on TNF-α production when dosed orally. Solubility was most likely not a major factor in this lack of oral efficacy as all of the six compounds except for **28k** had greater solubility in simulated gastric fluid than **1**, which shows >90% efficacy at inhibiting TNF-α production in the same model when dosed orally at 40 mg/kg.[31] As we had set improvement over **1** as a goal of this current study, we evaluated the remaining inhibitors only via the oral route. The β-methyl nitroarginine inhibitors, **28s** and **28t**, did not show inhibition of TNF-α production when dosed orally in the mouse, suggesting that the underpinnings of oral bioavailability in compounds such as Marimastat and **1** are more complex than the presence of steric bulk at the β-carbon of the P2′ side chain. Compounds **28o** and **28p** showed a nonsignificant 30% and 28% inhibition of TNF-α production after oral dosing. There may be some specific metabolism or efflux transport associated with the nitroarginine and sulfonylarginine groups as incorporated in the inhibitors studied in the present work. Efflux transport or low adsorption may be more likely than metabolic liability owing to the known metabolic stability of nitroarginine itself.[52]

Compound **28a** was evaluated in the zymosan-induced rat pleurisy model of inflammation. When **28a** was administered in a single 50 mg/kg sc bolus dose 10 min prior to zymosan injection, at 4 h a significant 30% ($P < 0.01$) reduction in total pleural cavity TNF-α was found (Table 5). For comparison, **1** at 80 mg/kg po showed a significant ($P < 0.001$) 89% inhibition of pleural TNF-α at 4 h compared to vehicle control.[35]

Conclusions

We have discovered potent and selective inhibitors of TACE in the *N*-hydroxyformamide class of prime-side inhibitors. By incorporating mimetics of the P2′ Arg of 26 kDa TNF-α into this class of TACE inhibitor, greatly increased aqueous solubility was observed. By selectively blocking the production of soluble 17 kDa TNF-α, our approach to TNF inhibition may be viewed as complimentary to that of agents which block both the 17 kDa as well as the membrane-associated 26 kDa forms. Therapeutic blockade of only the mature 17 kDa form could offer the advantages of allowing normal inflammatory responses to progress without potentially leading to immune suppression. Additionally, a small molecule approach to TNF blockade could provide better tolerability and patient compliance than with injectable therapies. Inhibitors in this class were shown to be effective in vivo at lowering systemic TNF-α levels in the LPS-challenged mouse as well as lowering TNF-α in the pleural cavity of zymosan challenged rats.

Compounds of the general formula **28** may thus be considered to be potent, selective inhibitors of TACE with significant aqueous solubility to allow for parenteral administration in acute settings.

Experimental Section

General. All commercial chemicals and solvents were reagent grade and were used without further purification unless otherwise specified. The following abbreviations have been used: tetrahydrofuran (THF), ethyl acetate (EtOAc), dimethyl sulfoxide (DMSO), dichloromethane (DCM), trifluoroacetic acid (TFA), dimethylformamide (DMF), methanol (MeOH), lithium diisopropylamide (LDA), 1,3-dimethyl 3,4,5,6-tetrahydro-2(1*H*)-pyrimidinone (DMPU), ethylenediamine tetracetic acid (EDTA), thin-layer chromatography (TLC), 1,3-dicylcohexylcarbodiimide (DCC), 1-(3-dimethylaminopropyl)-3-ethylcarbodiimide hydrochloride (EDC), tetrahydropyran-2-yl (THP), *t*-butoxycarbonyl (Boc), methanesulfonyl (Ms), triethylamine (TEA), diethyl phosphorylcyanide (DEPC), 4-methylmorpholine (NMM), and acetic acid (AcOH). Details of the general experimental procedures and instrumentation employed have been previously described.[53]

In Vitro. TACE SPA Assay.[43] Inhibition constants for inhibitors of TACE were determined in 96-well plates using a scintillation proximity assay (SPA). A tritium labeled, biotinylated peptide based on the cleavage sequence of 26kDa TNF-α (Biotin-SPLAQAVRSSSRTP*S-NH_2) was synthesized for substrate in these assays. Human TACE, isolated in a microsomal preparation from Mono Mac-6 monocytic leukemia cells, was diluted 1/25 into 10 mM HEPES, pH 7.5, for incubation with TACE substrate. After 1 h at 37 °C, substrate turnover was determined in the presence or absence of inhibitor using streptavidin SPA beads (Amersham). Percentage inhibition vs log [inhibitor] was plotted to determine the IC_{50} where $Ki = IC_{50}/(1 + [S]/Km)$.

MMP Assays.[42] Recombinant catalytic domains of MMP-1 and full length active MMP-3 were expressed and purified from *E. coli*. Enzymes were refolded in 200 mM NaCl, 50 mM Tris, 5 mM $CaCl_2$, 10 μM $ZnSO_4$, and 0.01% Brij 35, pH 7.6, for 1 h prior to the assay. The catalytic domain of proMMP-9 was purified from the media of baculovirus infected *T. ni* cells. Assays were run in a total volume of 0.180 mL of assay buffer containing 200 mM NaCl, 50 mM Tris, 5 mM $CaCl_2$, 10 μM $ZnSO_4$, and 0.01% Brij 35, pH 7.6. MMP-1, MMP-3, and MMP-9 concentrations were adjusted to 1.0 nM, 5 nM, and 0.1 nM, respectively. Enzymes were preincubated with inhibitor for 20 min at room temperature and the reactions were initiated with the addition of the fluorogenic substrate, Dnp-Pro-Cha-Gly-Cys(Me)-His-Ala-Lys(Nma)-NH_2. Dose responses were generated using eleven point 3-fold dilutions of the inhibitor. Product was measured using excitation and emission wavelengths of 343 and 450 nm, respectively.

Cellular Assay.[26] Inhibition of lipopolysaccharide (LPS)-induced TNF release was measured in human Mono Mac-6 cells.[44] Mono Mac-6 cells in RPMI 1640 media with 10% fetal bovine serum (FBS) were preincubated for 10 min with compounds **28a**−**u** and then stimulated with 10 ng/mL phorbol 12-myristate 13-acetate (PMA; Sigma Chemical Co.) and 30 ng/mL LPS (Sigma). After 2 h, TNF-α was measured in the media by ELISA kit (R&D Systems, Minneapolis, MN).

In Vivo. LPS−Induced TNF-α Release in Mice. Compounds were administered either via sc injection, dissolved in DMSO and added to a mixture of 0.9% NaCl and 30% Trappsol HPB-20 (CTD Inc., Gainsville, FL) for a final DMSO concentration of 1%, or by oral gavage (0.5% hydroxypropyl methylcellulose, 0.1% Tween 80 as a homogenized suspension). The sc dose was administered as a 0.2-mL solution and the oral suspension was administered by gavage at 5 mL/kg body weight, both given 10 min prior to LPS injection. C3H/hen female mice were injected ip with 0.2 mg/kg body weight of LPS in phosphate buffered saline and were killed 90 min after LPS injection by carbon dioxide asphyxiation. Blood was taken immediately from the inferior vena cava, and plasma was prepared and frozen at −80 °C. Plasma concentrations of TNF-α were measured by ELISA (R&D Systems, Minneapolis,

MN). TNF-α concentrations from $n = 7$ mice receiving test compound were compared to those from a control group receiving vehicle alone ($n = 7$).

Zymosan-Induced Rat Pleurisy. Male Lewis rats (Charles River Laboratories, Raleigh, NC) were dosed subcutaneously with **28a** (50 mg/kg; aqueous suspension with 5% EtOH, 5% propylene glycol, 10% Cremephore, and 10% Molecusol) 10 min prior to intrapleural injection of zymosan (Sigma Chemical Co.; 0.5 mg in 0.25 mL of H_2O). After 4 h, the pleural exudate was collected using a 16 ga. lavage needle and placed in a tube with EDTA, and cells were removed by centrifugation. Total TNF-α was measured in the pleural exudate by ELISA (Biosource International, Camarillo, CA) after spinning down the cells.

L−N^G-Nitroarginine 2-aminothiazole amide dihydrochloride (9). To a stirred solution of Na-Boc-L-Arg (5.00 g, 15.6 mmol) and 2-aminothiazole (1.72 g, 17.2 mmol) in dry DMF (16 mL) was added EDC (3.30 g, 17.2 mmol). The solution was stirred for 4 h then added to half-saturated NaCl solution and extracted with EtOAc (3×). The combined organic extracts were washed with 1 N $NaHSO_4$ (2×), 5% NaHCO3 (3×), and brine, and dried over $MgSO_4$. Filtration and concentration provided Nα-Boc-N^G-L-nitroarginine 2-aminothiazole amide as a sticky solid (2.28 g, 5.68 mmol, 36%). ^{1}H NMR (300 MHz, CD_3OD) δ 7.42 (d, $J = 3.6$ Hz, 1H), 7.10 (d, $J = 3.6$ Hz, 1H), 4.31 (m, 1H), 3.29 (m, 2H), 1.85 (m, 1H), 1.71 (m, 2H), 1.41 (s, 9H), 1.33 (m, 1H) ppm.

The Boc amino amide (2.28 g, 5.68 mmol) was dissolved in 5 mL of dry THF and treated with 5 mL of 4 N HCl in dioxane. After 3 h at ambient temperature, DCM was added and the precipitated product was filtered. The gummy solid was triturated with methanol/toluene to afford the title compound as a tan solid (1.63 g, 4.83 mmol, 85%). ^{1}H NMR (300 MHz, DMSO-d_6) δ 8.58 (bs, 4H), 7.99 (bs, 1H), 7.52 (d, $J = 3.6$ Hz, 1H), 7.31 (d, $J = 3.6$ Hz, 1H), 6.4−5.9 (bs, 2H), 4.08 (m, 1H), 3.17 (bs, 2H), 1.83 (m, 2H), 1.53 (m, 2H) ppm. ESIMS *m*/*z* (pos. ion.) 302 $(M+H)^+$; (neg. ion) 300 $(M-H)^+$. Anal. ($C_9H_{15}N_7O_3S\cdot 2HCl\cdot 0.25C_4H_8O$) C, H, N, S.

L-N^G-(2-Pyridylsulfonyl)arginine 2-aminothiazole amide hydrochloride (11). Boc-L-Arg (2.00 g, 7.29 mmol) in 40 mL of acetone/H_2O (80:20) at 0 °C was brought to pH 11−12 by the addition of 3 N NaOH solution. 2-Pyridylsulfonyl chloride (3.2 g, 18.2 mmol) in acetone was added dropwise over 30 min during which time the pH was maintained at 11−12 with additional 3 N NaOH. After 5 h at 0 °C, the pH was adjusted to 6 with 8 N HCl, and the acetone was removed in vacuo. The resulting oily suspension was acidified to pH 3−4 with 0.5 N citric acid and extracted with EtOAc (3×), washed with ice cold 0.2 N HCl (3×) and brine, and dried over Na_2SO_4. Filtration and concentration provided Nα-Boc-N^G-L-(2-pyridylsulfonyl)arginine as a yellow glass (1.54 g, 3.71 mmol, 51%). ESIMS *m*/*z* 416 $(M+H)^+$, 438 $(M+Na)^+$, 316 $(MH-Boc)^+$. The amino acid (361 mg, 0.869 mmol) and 2-aminothiazole (174 mg, 1.74 mmol) were dissolved in 1.2 mL of anhydrous DMF. EDC (183 mg, 0.956 mmol) was added, and the reaction mixture was heated to 40 °C for 40 h. The cooled reaction mixture was poured into H_2O and extracted with hexanes/EtOAc (1:1) (4×) to provide Nα-Boc-N^G-L-(2-pyridylsulfonyl)-arginine 2-aminothiazole amide as a white foam (189 mg, 0.38 mmol, 44%). ^{1}H NMR (400 MHz, CD_3OD) δ 8.56 (d, $J = 4.8$ Hz, 1H), 7.94 (d, $J = 3.6$ Hz, 2H), 7.45 (m, 1H), 7.42 (d, $J = 3.6$ Hz, 1H), 7.11 (d, $J = 3.2$ Hz, 1H), 4.3−4.1 (m, 1H), 3.3−3.2 (m, 2H), 1.8−1.4 (m, 4H), 1.42 (s, 9H) ppm. ESIMS *m*/*z* 498 $(M+H)^+$, 520 $(M+Na)^+$, 398 $(MH-Boc)^+$. The Boc amino amide (189 mg, 0.380 mmol) was taken up in 1 mL of 4 N HCl in dioxane, and after 1 h it was concentrated in vacuo and repeatedly stripped from MeOH/toluene to provide the title compound as a white foam contaminated with a small amount of dioxane (169 mg, 0.360 mmol, 95%). ^{1}H NMR (400 MHz, DMSO-*d6*) δ 8.54 (d, $J = 4.8$ Hz, 1H), 8.50 (bs, 2H), 7.93 (m, 1H), 7.81 (d, $J = 7.6$ Hz, 1H), 7.51 (m, 2H), 7.29 (d, $J = 4.0$ Hz, 1H), 7.25 (bs, 1H), 7.0−6.6 (bs, 4H), 4.02 (m, 1H), 3.08 (m, 2H), 1.78 (m, 2H), 1.45 (m, 2H) ppm. ESIMS *m*/*z* 398 $(M+H)^+$, 420 $(M+Na)^+$.

(2*S*)-2-[(*tert*-Butoxycarbonyl)amino]-5-({(*Z*)-(methylsulfanyl)[(methylsulfonyl)imino]methyl}amino)pentanoic acid (13). An aqueous solution of NaOH (3.1 mL, 2.0 N) was added to a mixture of Nα-Boc-L-ornithine (1.30 g, 5.59 mmol) and MsN=C(SMe)$_2$ (1.67 g, 8.38 mmol) in 30 mL of absolute ethanol and stirred at 60−65 °C. After 15 h, the reaction mixture was refluxed for a further 2 h. The ethanol was removed in vacuo and the resulting slurry was added to H_2O and extracted with ether (3×), acidified to pH 1 with 1 N HCl, and extracted with EtOAc (4×). The combined EtOAc layers were washed with H_2O and brine and dried over $MgSO_4$. Filtration and concentration provided **13** (2.40 g, 112%) as a white oily foam, contaminated by a small amount of MsN=C(SMe)$_2$. ^{1}H NMR (400 MHz, DMSO-d_6) (major rotamer) δ 12.4 (bs, 1H), 7.8 (bs, 1H), 7.06 (bd, $J = 7.2$ Hz, 1H), 3.83 (m, 1H), 3.4 (bs, 1H), 3.24 (m, 2H), 2.86 (s, 3H), 2.44 (s, 3H), 1.54 (m, 4H), 1.34 (s, 9H) ppm. ESIMS *m*/*z* (pos. ion) 384 $(M+H)^+$, 406 $(N+Na)^+$, (neg. ion) 382 $(M-H)^+$.

***tert*-Butyl(1*S*)-4-({(*Z*)-(methylsulfanyl)[(methylsulfonyl)-imino]methyl}amino)-1-[(1,3-thiazol-2-ylamino)carbonyl]butylcarbamate (14).** Compound **13** (3.03 g, 7.90 mmol) and TEA (0.799 g, 7.90 mmol, 1.10 mL) were dissolved in DMF (40 mL) and cooled to −23 °C. *i*-BuOCOCl (1.08 g, 1.03 mL, 7.90 mmol) was added dropwise with stirring. After 45 min, 2-aminothiazole (0.791 g, 7.9 mmol) was added, and stirring continued for a further 30 min at −23 °C. The reaction mixture was allowed to warm to ambient temperature over 15 h then added to a half-saturated NaCl solution and extracted with EtOAc (3×). The combined organic layers were washed with 1 N $NaHSO_4$, 5% $NaHCO_3$, and brine, and dried over $MgSO_4$. Purification on SiO_2 (hexanes/EtOAc 4:1, then 100% EtOAc) provided amide **14** as a white foam (3.30 g, 7.09 mmol, 90.%). ^{1}H NMR (400 MHz, $CDCl_3$) δ 7.9 (bs, 1H), 7.54 (d, $J = 3.6$ Hz), 7.01 (d, $J = 3.6$ Hz, 1H), 5.25 (bs, 1H), 4.45 (m, 1H), 3.30 (m, 2H), 2.98 (s, 3H), 2.35 (s, 3H), 1.95 (m, 1H), 1.73 (m, 2H), 1.65 (m, 2H), 1.44 (s, 9H) ppm. ESIMS *m*/*z* 466 $(M+H)^+$, 488 $(M+Na)^+$.

(2*S*)-2-Amino-5-({(*E*)-amino[(methylsulfonyl)imino]-methyl}amino)-*N*-(1,3-thiazol-2-yl)pentanamide hydrochloride (15). To a 0 °C solution of isothiourea **14** (3.30 g, 7.09 mmol) in 11 mL of a 2.0 M solution of ammonia in methanol was added $AgNO_3$ (1.32 g, 7.80 mmol) dissolved in MeCN (5 mL) over 10 min. A yellow precipitate of AgSMe formed, and the reaction mixture was stirred as it warmed to ambient temperature over 2 h. Volatiles were removed in vacuo and the resulting mixture was triturated in EtOAc. The AgSMe was removed by filtration through a glass frit. The filtrate was concentrated and placed under high vacuum overnight to provide methanesulfonyl arginine derivative **Nα-Boc 15** as a white foam (3.04 g, 7.00 mmol, 99%). ^{1}H NMR (300 MHz, DMSO-d_6) δ 12.18 (s, 1H), 7.50 (d, $J = 3.6$ Hz, 1H), 7.24 (d, $J = 3.6$ Hz, 1H), 7.0−6.4 (m, 2H), 4.06 (m, 1H), 3.07 (m, 2H), 2.77 (s, 3H), 1.7−1.4 (m, 4H), 1.39 (s, 9H) ppm. ESIMS *m*/*z* 435 $(M+H)^+$, 464 $(M+Na)^+$, 335 $(MH-Boc)^+$.

The Boc amino amide (3.04 g, 7.00 mmol) was dissolved in 3 mL of methanol and 5 mL of 4 N HCl in dioxane. After 2 h volatiles were removed in vacuo, and the product was repeatedly stripped from a mixture of methanol and toluene to provide **15** as a white foam containing some toluene (2.83 g, 8.47 g, 120%). ^{1}H NMR (400 MHz, DMSO-d_6) δ 8.58 (bs, 6H), 7.51 (d, $J = 3.6$, Hz, 1H), 7.31 (d, $J = 3.6$ Hz, 1H), 7.16 (m, 1H), 6.8−6.5 (bs, 1H), 4.09 (m, 1H), 3.15 (s, 3H), 3.0−2.6 (bs, 3H), 1.82 (m, 2H), 1.50 (m, 2H) ppm. ESIMS *m*/*z* 335 $(M+H)^+$.

***tert*-Butyl (2*S*,3*R*)-2-{[(benzyloxy)carbonyl]amino}-3-methyl-4-pentenoate (17).** Acid **16a** (25.2 g, 112 mmol) was stirred at 80 °C in a solution of 2 N NaOH (112 mL) for 1.5 h. The reaction mixture was cooled to 0 °C and an additional 112 mL of 2 N NaOH was added followed by benzyl chloroformate (18 mL, 126 mmol). After 45 min stirring at 0 °C, the reaction mixture was allowed to warm to ambient temperature over 5 h and the mixture was poured into 150 mL of water. The solution was basified with additional NaOH solution and extracted with ether, and the ether layer was discarded. The aqueous phase was acidified with 6 N HCl to pH 1 and

extracted with ether (3×). The combined organic extracts were dried over $MgSO_4$, filtered, and concentrated in vacuo to afford 22.6 g (86.2 mmol, 77%) of *tert*-butyl (2*S*,3*R*)-2-{[(benzyloxy)-carbonyl]amino}-3-methyl-4-pentenoic acid as a clear oil. ^{1}H NMR (300 MHz, $CDCl_3$) δ 8.39 (bs, 1H), 7.35 (m, 5H), 5.71 ddd, 1H, 5.13 (m, 2H), 4.43 (dd, 1H), 2.74 (m, 1H), 1.10 (d, 3H) ppm. ESIMS *m*/*z* 264 $(M+H)^+$, 286 $(M+Na)^+$.

tert-Butyl (2*S*,3*R*)-2-{[(benzyloxy)carbonyl]amino}-3-methyl-4-pentenoic acid (20.6 g, 78.2 mmol) was dissolved in toluene (156 mL) and heated to 80 °C. Dimethylformamide di-*tert*-butyl acetal (DMF-DBA) was added over 30 min., and the reaction solution was maintained at 80 °C for a further 45 min. when an additional 10 mL of DMF-DBA was added. After an additional 1 h, the mixture was allowed to cool to ambient temperature and was diluted with ether. The reaction mixture was washed with water, 5% $NaHCO_3$, and brine, and dried ($MgSO_4$). Filtration and concentration provided **17** as a clear oil (15.5 g, 48.5 mmol, 62%). ^{1}H NMR (300 MHz, $CDCl_3$) δ 7.30 (m, 5H), 5.75 (m, 1H), 5.28 (bd, 1H), 5.07 (m, 2H), 4.27 (bd, 1H), 2.63 (m, 1H), 1.44 (s, 9H), 1.04 (d, 3H) ppm.

***tert*-Butyl ((2*S*,3*R*)-2-{[(benzyloxy)carbonyl]amino}-5-hydroxy-3-methylpentanoate (18).** To a 0 °C solution of 2,3-dimethyl-2-butene (43.2 mL, 1.0 M in THF) was added dropwise over 20 min a solution of borane in THF (43.2 mmol, 1.0 M). After the solution was stirred an additional 60 min at 0 °C, **17** (13.1 g, 41.2 mmol) in 20 mL of THF was added dropwise and the resulting solution was allowed to warm to ambient temperature over 1 h. The solution was recooled to 0 °C and excess borane was quenched by the cautious addition of 6 mL of 1:1 THF/ethanol followed by 40 mL of pH 7.00 phosphate buffer then 40 mL of 30% H_2O_2. After the reaction mixture stirred at ambient temperature for 14 h, it was partially concentrated, added to brine, and extracted with ether (3×). The combined organic layers were washed with ice-cold saturated aqueous $Na_2S_2O_5$ solution (4×), water, and brine, and dried over $MgSO_4$. Filtration and concentration provided a crude product that was purified on SiO_2 (hexanes/EtOAc 3:2) to afford compound **18** (12.3 g, 36.7 mmol, 89%). ^{1}H NMR (400 MHz, $CDCl_3$) δ 7.34 (m, 5H), 5.40 (bd, 1H), 5.09 (s, 2H), 4.11 (m, 1H), 3.78 (m, 1H), 3.65 (m, 1H), 2.22 (m, 1H), 1.7−1.6 (bs, 1H), 1.63 (m, 2H), 1.45 (s, 9H), 0.84 (d, 3H) ppm. ESIMS *m*/*z* 338 $(M+H)^+$, 360 $(M+Na)^+$.

***tert*-Butyl ((2*S*,3*R*)-2-{[(benzyloxy)carbonyl]amino}-5-azido-3-methylpentanoate (19).** Alcohol **18** (12.3 g, 36.4 mmol) was dissolved in 60 mL of DCM and 8.8 mL of pyridine and cooled to 0 °C. Methanesulfonyl chloride (4.59 g, 40.1 mmol, 3.10 mL) was added via syringe, and the resulting solution was allowed to stir for 14 h then washed with 1 N HCl and brine, and dried over $MgSO_4$. Filtration and concentration afforded the crude mesylate which was taken up in 50 mL of dry DMF, and LiN_3 (5.36 g, 109 mmol) was added and the reaction mixture was warmed to 50 °C for 3 h. The reaction mixture was added to water and extracted three times with ether. The combined organic layers were dried over $MgSO_4$, filtered, and concentrated to give a crude azide (10.3 g) which was purified on SiO_2 (hexanes/EtOAc 8:1) to provide azide **19** as an oil (9.40 g, 25.8 mmol, 71%). ^{1}H NMR (400 MHz, $CDCl_3$) δ 7.34 (m, 5H), 5.28 (bd, 1H), 5.09 (s, 2H), 4.31 (m, 1H), 3.39 (m, 2H), 2.18 (m, 1H), 1.84 (d, 3H), 1.72 (m, 1H), 1.45 (s, 9H), 1.40 m, 1H) ppm. ESIMS *m*/*z* 385 $(M+Na)^+$, 329 $(M+Na-C_4H_8)^+$.

***tert*-Butyl ((2*S*,3*R*)-2-{[(benzyloxy)carbonyl]amino}-5-amino-3-methylpentanoate (20).** *tert*-Butyl ((2*S*,3*R*)-2-{[(benzyloxy)carbonyl]amino}-5-azido-3-methylpentanoate (**19**, 1.02 g, 2.81 mmol) was dissolved in 10 mL of methanol and TEA (0.39 mL, 2.8 mmol), and hydrogenated at 30 psi over 0.05 g of Lindlar catalyst. After 4 h the catalyst was removed by filtration, and the filtrate was concentrated to give the primary amine **20** as a clear oil (0.94 g, 2.80 mmol, 100%). ^{1}H NMR (400 MHz, DMSO-d_6) δ 7.53 (bd, 1H), 7.45 (bs, 1H), 7.33 (m, 5H), 7.4−6.5 (bs, 2H), 5.02 (m, 2H), 4.00 (m, 1H), 1.98 (m, 1H), 1.6−1.1 (m, 2H), 1.37 (s, 9H), 0.82 (s, 3H) ppm. ESIMS *m*/*z* 379 $(M+H)^+$, 323 $(M+H-C_4H_8)^+$.

(2*S*,3*R*)-2-{[(Benzyloxy)carbonyl]amino}-3-methyl-5-({(*Z*)−(methylsulfanyl)[(methylsulfonyl)imino]methyl}-amino)pentanoic acid (21). Amine **20** (0.940 g, 2.80 mmol) was dissolved in 25 mL of 95% ethanol, and aqueous NaOAc solution was added (1.0 mL, 3.0 M, 3.0 mmol). Dimethyl methylsulfonyldithioimidocarbonate (0.612 g, 3.07 mmol) was added, and the reaction mixture was refluxed for 48 h. The ethanol was removed in vacuo, and the resulting mixture was extracted with ether. The ether extracts were washed with water, 1 M $NaHSO_4$ (2×), 5% $NaHCO_3$, and brine and dried over $MgSO_4$. Filtration and concentration afforded the crude isothiourea (ESIMS *m*/*z* 510 $(M+Na)^+$) which was taken up in 12 mL of acid cocktail (CF_3COOH/thioanisole/water/*i*-Pr_3-SiH 88:5:5:2) and allowed to stand at ambient temperature for 1 h. The reaction mixture was concentrated then placed under high vacuum for 1 h. The resulting oil was taken up in 50 mL of 5% $NaHCO_3$ and sonicated, then extracted with ether (3×), acidified with 6 N HCl, extracted with DCM (4×), and dried over $MgSO_4$. Filtration provided the desired acid (**21**) contaminated by 20% methylsulfonyldithioimidocarbonate (0.943 g containing 1.98 mmol of **21**, 71% from **20**). ^{1}H NMR (400 MHz, $CDCl_3$) δ 8.6 (bs, 2H), 7.95 (bs, 1H), 7.33 (m, 5H), 5.41 (d, J = 8.8, 1H), 5.09 (m, 2H), 4.47 (dd, J = 9.2, 3.6 Hz, 1H), 3.5−3.3 (m, 2H), 2.99 (s, 3H), 2.36 (s, 3H), 2.2−2.0 (m, 1H), 1.8−1.7 (m, 1H), 1.6−1.5 (m, 1H), 0.91 (d, J = 6.8, 3H) ppm. ESIMS *m*/*z* 432 (M+H)+, 863 $(2M+H)^+$.

Benzyl (1*S*,2*R*)-4-({(*E*)-amino[(methylsulfonyl)imino]-methyl}amino)-2-methyl-1-[(1,3-thiazol-2-ylamino)carbonyl]butylcarbamate (22). Isobutyl chloroformate (0.262 g, 1.92 mmol, 0.25 mL) was added with stirring to a −23 °C solution of acid **21** (0.828 g, 1.92 mmol) and TEA (0.266 mL, 1.92 mmol) in 5 mL of anhydrous DMF. After 1 h, 2-amino-thiazole (0.192 g, 1.92 mmol) was added, and the reaction mixture was allowed to warm to ambient temperature over 16 h. The solution was added to 50%-saturated NaCl solution and extracted with EtOAc (4×). The combined organic extracts were washed with 1 N HCl (2×), 5% $NaHCO_3$, and brine and dried over $MgSO_4$. Purification on SiO_2 (hexanes/EtOAc 1:2 then 1:5) afforded benzyl (1*S*,2*R*)-2-methyl-4-({(*Z*)-(methylsulfanyl)[(methylsulfonyl)imino]methyl}amino)-1-[(1,3-thiazol-2-ylamino)carbonyl]butylcarbamate as a white glassy solid free from contamination by methylsulfonyldithioimidocarbonate (0.608 g, 1.18 mmol, 44% for three steps). ^{1}H NMR (400 MHz, $CDCl_3$) δ 12.0 (bs, 1H), 7.9 (bs, 1H), 7.56 (d, J = 3.6 Hz, 1H), 7.32 (m, 5H), 6.99 (d, J = 3.6 Hz, 1H), 5.85 (d, J = 8.8 Hz, 1H), 5.11 (AB, J = 12 Hz, 2H), 4.67 (m, 1H), 3.2−3.2 (m, 2H), 2.96 (s, 3H), 2.31 (s, 3H), 2.10 (m, 1H), 1.8 (m, 1H), 1.5 (m, 1H), 0.92 (d, J = 6.8 Hz, 3H) ppm. ESIMS *m*/*z* 514 $(M+H)^+$, 536 $(M+Na)^+$.

The isothiourea (0.608 g, 1.18 mmol) was dissolved in 6.0 mL of a 2.0 M methanolic ammonia solution and cooled to 0 °C. A solution of $AgNO_3$ (0.220 g, 1.30 mmol) in methanol (3 mL) was added dropwise over 5 min, and the reaction mixture was allowed to come to ambient temperature over 1.5 h. Ethyl acetate was added, and the mixture was filtered through Celite diatomaceous earth and concentrated in vacuo to provide the title compound as a glassy solid (0.651 g, 1.35 mmol, 114%). ^{1}H NMR (400 MHz, CD_3OD) δ 7.45 (d, J = 3.6 Hz, 1H), 7.4−7.0 (m, 6H), 5.08 (AB, J = 12.4 Hz, 2H), 4.43 (m, 1H), 3.3−3.2 (m, 2H), 2.84 (s, 3H), 2.2−2.1 (m, 1H), 1.7−1.6(m, 1H), 1.5−1.4 (m, 1H), 0.94 (d, J = 6.0 Hz, 3H) ppm. ESIMS *m*/*z* 483 $(M+H)^+$, 505 $(M+Na)^+$.

[((3*R*,4*S*)-4-{[(Benzyloxy)carbonyl]amino}-4-carboxy-3-methylbutyl)amino](imino)methanaminium nitrate ((3R) 3-Methyl L-arginine nitric acid salt, 24). To a solution of amine **20** (0.906 mg, 2.69 mmol) and TEA (0.8 mL, 5.7 mmol) in DMF (5 mL) was added 3,5-dimethylpyrazole-1-carboxamidine nitrate (0.542 g, 2.69 mmol). After 72 h at ambient temperature, the volatiles were removed under high vacuum. The oily residue was taken up in 40 mL of EtOAc, sonicated to a fine suspension, and triturated by stirring for 1 h. Filtration through glass provided the title compound as a white solid displaying very broad peaks in the NMR spectrum (0.856 g, 1.94 mmol, 72%). ^{1}H NMR (400 MHz, DMSO-d_6) δ

7.52 (bd, $J = 3.6$ Hz, 1H), 7.45 (bs, 1H), 7.33 (m, 5H), 7.2−6.6 (bs, 4H), 5.00 (AB, $J = 12$ Hz, 2H), 4.00 (m, 1H), 3.2−3.0 (m, 2H), 2.1−1.9 (m, 1H), 1.6−1.4 (m, 1H), 1.37 (s, 9H), 1.2 (m, 1H), 0.82 (bd, $J = 6.4$ Hz, 3H) ppm. ESIMS *m/z* 379 $(M+H)^+$, 323 $(M+H-C_4H_8)^+$.

(2*S*,3*R*)-2-[(*tert*-Butoxycarbonyl)amino]-5-{[imino(2-oxido-2-oxohydrazino)methyl]amino}-3-methylpentanoic acid ((3R) N^{α}-Boc-N^{γ}-nitro-3-methyl L-arginine, 25). (3R)-3-Methyl l-arginine derivative **24** (0.856 g, 1.94 mmol) was dissolved in 10 mL of methanol and stirred with 1,4-cyclobutadiene (2 mL) and 10% Pd/C (80 mg) at reflux for 1 h. The cooled mixture was filtered through Celite diatomaceous earth and concentrated in vacuo to provide the free amine (0.599 g of white solid, ESIMS *m/z* 245 $(M+H)^+$, 189 $(M+H-C_4H_8)^+$ which was dissolved in 5 mL of 95% TFA in water. After 1 h the volatiles were removed, and the resulting oil was repeatedly stripped from ethanol, EtOAc, and toluene to provide (3R)-3-methyl L-arginine as an oil (1.04 g; ESIMS *m/z* 189 $(M+H)^+$, 172 $(M+H-NH_3)^+$. The crude oil was dissolved in 1 mL of concentrated H_2SO_4 and cooled in an ice−acetone bath. A pre-cooled (−15 °C) mixture of fuming H_2SO_4 (1.5 mL) and fuming nitric acid (1.0 mL) was added dropwise to the stirred solution. After 2 h at −10 to −15 °C, the cooling bath was removed, and ice was added to the reaction mixture. Ammonium hydroxide solution (30%) was added cautiously to bring the reaction mixture to pH 8, then the pH was adjusted to 5 with glacial acetic acid. The volatiles were removed in vacuo to provide a yellow solid which was triturated for 1 h with methanol. Filtration through glass provided a crude yellow solid (ESIMS *m/z* 234 $(M+H)^+$) which was dissolved in 15 mL of 5% $NaHCO_3$ and concentrated to dryness (2×). The resulting mixture was taken up in 10 mL of fresh 5% $NaHCO_3$ and THF (10 mL), and di(*tert*-butyl) dicarbonate (0.465 g) was added. After 18 h, 5 g of $NaHCO_3$ was added along with additional di(*tert*-butyl) dicarbonate (0.05 g). After an additional 72 h, the reaction mixture was extracted with ether (2×). The aqueous layer was acidified with 6 N HCl to pH 1, saturated with NaCl, and extracted with DCM (3×). The combined organic layers were dried over $MgSO_4$, filtered, and concentrated to give **25** as a yellow foam (0.125 g, 0.375 mmol, 19% from **24**). ^{1}H NMR (400 MHz, $CDCl_3$) δ 10.8−10.6 (bs, 2H), 8.68 (bs, 1H), 7.9−7.5 (bs, 1H), 5.38 (d, $J = 8.0$ Hz, 1H), 4.45 (d, $J = 7.2$ Hz, 1H), 3.8−3.6 (bs, 1H), 3.4−3.2 (bs, 1H), 2.3−2.1 (bs, 1H), 1.7−1.6 (m, 1H), 1.5−1.4 (m, 1H), 1.43 (s, 9H), 0.86 (d, $J = 6.8$ Hz, 3H) ppm. ESIMS *m/z* 334 $(M+H)^+$, 356 $(M+Na)^+$, 278 $(M+H-C_4H_8)^+$.

***tert*-Butyl (1*S*,2*R*)-4-{[imino(2-oxido-2-oxohydrazino)-methyl]amino}-2-methyl-1-[(1,3-thiazol-2-ylamino)carbonyl]butylcarbamate (26).** To a solution of acid **25** (0.123 g, 0.369 mmol) and TEA (0.051 mL, 0.369 mmol) in DMF (1 mL) at −23 °C was added isobutyl chloroformate (0.048 mL, 0.369 mmol). After 40 min 2-aminothiazole (0.041 g, 0.406 mmol) was added, and the reaction mixture was allowed to warm to ambient temperature over 2 h. The reaction mixture was poured into 50%-saturated NaCl solution and extracted with EtOAc (4×). The combined organic layers were washed with 1 N HCl (2×), 5% $NaHCO_3$, and brine, and dried over $MgSO_4$. Purification on SiO_2 (hexanes/EtOAc 1:5 then 100% EtOAc) gave the title compound as a yellow foam (0.101 g, 0.243 mmol, 66%). ^{1}H NMR (400 MHz, CD_3OD) δ 7.35 (d, $J = 3.6$ Hz, 1H), 7.03 (d, $J = 3.6$ Hz, 1H), 6.85 (bd, $J = 8.0$ Hz, 0.7 H (NH partially exchanged)), 4.31 (m, 1H), 3.25 (M, 2H), 2.1−2.0 (m, 1H), 1.7−1.5 (m, 1H), 1.4 (m, 1H), 1.36 (s, 9H), 0.86 (d, $J = 6.8$ Hz, 3H) ppm. ESIMS *m/z* 416 $(M+H)^+$, 360 $(M+H-C_4H_8)^+$, 316 $(M+H-Boc)^+$.

General Procedure for the Preparation of *N*-Hydroxy Formamides 28a−u. Diethyl phosphorylcyanide (DEPC, 1.1 equiv) was added dropwise to a solution of acid **7j−t** (1.0 equiv) and NMM (1.1 equiv) in DMF (0.2−0.5 M) at 0 °C. After 0.5 h, the mixture was allowed to warm to ambient temperature over 0.5 h. To this solution was added amino amide (**9**, **11**, **15**, **23**, or **27**, 1.1 equiv) and additional NMM (2.2 equiv). After 12−16 h at 23−40 °C the reaction mixture was added to 50%-saturated NaCl solution and extracted with EtOAc (3×). The combined organic layers were washed with pH 7.0 phosphate buffer and brine and dried over $MgSO_4$. Purification on SiO_2 (DCM/MeOH 95:5) resulted in an oil which was taken up in 80% aqueous AcOH and heated at 40 °C for 16−20 h. The compound was isolated by removal of the volatiles in vacuo and trituration with DCM and ether followed by filtration and drying of the amorphous solid under vacuum at 50 °C.

Alternatively, pentafluorophenyl ester **7n** (1 equiv) was dissolved in DMF and stirred with either **23** or **27** (1.1 equiv) at 40 °C for 2−5 h. Workup and purification were identical to those of the DEPC coupling procedure (vide supra).

(2*R*,3*S*)-*N*-{(1*R*)-4-Nitroguanyl-1-[(1,3-thiazol-2-ylamino)carbonyl]butyl}-3-[formyl(hydroxy)amino]-2-isobutylhexanamide (28a). White amorphous solid, 33%. ^{1}H NMR (400 MHz, DMSO-d_6, mixture of formamide rotamers) δ 12.14 (s, 1H), 9.70 (s, 0.33H), 9.44 (s, 0.67H), 8.6−8.4 (bs, 1H), 8.42 (m, 1H), 8.34 (s, 0.33H), 8.2−7.6 (bs, 1H), 7.94 (s, 0.67H), 7.46 (d, $J = 3.2$ Hz, 1H), 7.20 (d, $J = 3.2$ Hz, 1H), 4.48 (m, 1H), 4.16 (m, 0.33H), 3.47 (m, 0.67H), 3.16 (m, 2H), 2.66 (m, 1H), 1.8−1.0 (m, 11H), 0.85 (d, $J = 6.4$ Hz, 3H), 0.83−0.72 (m, 6H) ppm. ESIMS *m/z* 515 $(M+H)^+$, 537 $(M+Na)^+$. $\lambda_{max} = 269.0$ nm. Anal. ($C_{20}H_{34}N_8O_6S$) C, H, N.

(2*R*)-5-Nitroguanyl-2-({(2*R*,3*S*)-2-(cyclohexylmethyl)-3-cyclopropyl-3-[formyl(hydroxy)amino]propanoyl}-amino)-*N*-(1,3-thiazol-2-yl)pentanamide (28b). White amorphous solid, 46%. ^{1}H NMR (400 MHz, CD_3OD, mixture of formamide rotamers) δ 8.31 (s, 0.15H, partially exchanged NH), 8.24 (m, 0.1H, partially exchanged NH), 7.89 (s, 0.33H), 7.87 (s, 0.1H, partially exchanged NH), 7.71 (s, 0.67H), 7.41 (m, 1H), 7.10 (m, 1H), 4.64 (m, 1H), 3.6−3.4 (m, 0.33H), 3.25 (m, 0.67H), 3.20 (m, 2H), 2.91 (t, $J = 10$ Hz, 0.5H), 2.89 (t, $J = 10$ Hz, 0.5H), 2.0−1.4 (m, 12H), 1.3−1.0 (m, 5H), 1.0−0.7 (m, 2H), 1.7−0.3 (m, 2H), 0.3−0.1 (m, 1H) ppm. ESIMS *m/z* 553 $(M+H)^+$, 575 $(M+Na)^+$. λ_{max} 269 nm. Anal. ($C_{23}H_{36}N_8O_6S\cdot{}^1/_2H_2O$) C, H, N, S.

(2*R*,3*S*)-*N*-{(1*S*)-4-Nitroguanyl -1-[(1,3-thiazol-2-ylamino)carbonyl]butyl}-3-[formyl(hydroxy)amino]-2-[(5-methyl-2-thienyl)methyl]hexanamide (28c). Tan solid, 30%. ^{1}H NMR (400 MHz, DMSO-d_6, mixture of formamide rotamers) δ 11.99 (bs, 1H), 9.87 (s, 0.33H), 9.57 (s, 0.67H), 8.6−8.4 (bs, 1H), 8.44 (m, 1H), 8.40 (s, 0.33H), 8.2−7.6 (bs, 2H), 8.01 (s, 0.67H), 7.48 (d, $J = 3.2$ Hz, 1H), 7.23 (d, $J = 3.2$ Hz, 1H), 6.48 (s, 1H), 6.32 (s, 1H), 4.57 (m, 1H), 4.28 (m, 0.33H), 3.63 (m, 0.67H), 3.14 (m, 2H), 2.9−2.7 (m, 3H), 2.03 (s, 3H), 1.8−1.5 (m, 4H), 1.42 (m, 1H), 1.4−1.0 (m, 3H), 0.78 (m, 3H) ppm. ESIMS *m/z* 569 $(M+H)^+$, 591 $(M+Na)^+$. λ_{max} 269 nm. Anal. ($C_{22}H_{32}N_8O_6S_2\cdot{}^1/_3H_2O$) C, H, N, S.

(2*R*,3*S*)-*N*-{(1*S*)-4-Nitroguanyl -1-[(1,3-thiazol-2-ylamino)carbonyl]butyl}-2-(cyclohexylmethyl)-3-[formyl(hydroxy)amino]hexanamide (28d). White amorphous solid, 45%. ^{1}H NMR (400 MHz, DMSO-d_6, mixture of formamide rotamers) δ 12.11 (bs, 1H), 9.65 (s, 0.33H), 9.39 (s, 0.67H), 8.50 (bs, 1H), 8.44 (m, 1H), 8.30 (s, 0.33H), 8.2−7.6 (bs, 2H), 7.91 (s, 0.67H), 7.44 (d, $J = 3.6$ Hz, 1H), 7.18 (d, $J = 3.2$ Hz, 1H), 4.53 (m, 1H), 4.13 (t, $J = 11.2$ Hz, 0.33H), 3.43 (t, $J = 12$ Hz, 0.67H), 3.14 (m, 2H), 2.63 (m, 1H), 1.88 (m, 1H), 1.8−1.3 (m, 11H), 1.3−1.0 (m, 7H), 0.9−0.6 (m, 5H) ppm. λ_{max} 269 nm. ESIMS *m/z* 555 $(M+H)^+$, 577 $(M+Na)^+$. Anal. ($C_{23}H_{38}N_8O_6S\cdot{}^1/_4H_2O$) C, H, N, S.

(2*R*,3*S*)-*N*-{(1*S*)-4-Nitroguanyl -1-[(1,3-thiazol-2-ylamino)carbonyl]butyl}-3-[formyl(hydroxy)amino]-4-methyl-2-[(4-methylcyclohexyl)methyl]pentanamide (28e). White amorphous solid, 55%. ^{1}H NMR (400 MHz, DMSO-d_6, mixture of formamide rotamers and *cis*/*trans* 1,4-dialkylcyclohexane isomers) δ 12.10 (bs, 1H), 9.60 (m, 0.33H), 9.40 (m, 0.67H), 8.48 (m, 2H), 8.32 (s, 0.2H), 8.29 (s, 0.1H), 8.2−7.6 (m, 2H), 7.90 (s, 0.7H), 7.44 (d, $J = 3.6$ Hz, 1H), 7.19 (m, 1H), 4.53 (m, 2H), 4.08 (m, 0.33H), 3.37 (m, 0.67H), 3.12 (m, 2H), 2.91 (m, 1H), 2.0−1.1 (m, 13H), 0.96 (d, $J = 6.4$ Hz, 3H), 0.9−0.6 (m, 10H) ppm. λ_{max} 269 nm. ESIMS *m/z* 569 $(M+H)^+$, 591 $(M+Na)^+$. Anal. ($C_{24}H_{40}N_8O_6S\cdot{}^2/_3H_2O$) C, H, N, S.

(2*R*,3*S*)-*N*-{(1*S*)-4-Nitroguanyl -1-[(1,3-thiazol-2-ylamino)carbonyl]butyl}-3-[formyl(hydroxy)amino]-2-[(4-methylcyclohexyl)methyl]hexanamide (28f). White amor-

phous solid, 48%. ^{1}H NMR (400 MHz, DMSO-d_6, mixture of formamide rotamers and *cis/trans* 1,4-dialkylcyclohexane isomers) δ 12.10 (bs, 1H), 9.65 (bs, 0.33H), 9.42 (bs, 0.67H), 8.45 (m, 2H), 8.33 (s, 0.2H), 8.30 (s, 0.1H), 8.2−7.6 (bs, 2H), 7.92 (m, 0.67H), 7.44 (s_{app}, 1H), 7.18 (s_{app}, 1H), 4.51 (m, 1H), 4.13 (m, 0.33H), 3.35 (m, 0.67H), 3.15 (m, 2H), 2.63 (m, 1H), 1.0−0.9 (m, 16H), 0.9−0.8 (m, 10H) ppm. λ_{max} 269 nm. ESIMS *m/z* 569 $(M+H)^+$, 591 $(M+Na)^+$. Anal. ($C_{24}H_{40}N_8O_6S\cdot{}^2/_3H_2O$) C, H, N, S.

(2*R*,3*S*)-*N*-{(1*S*)-4-(2-Pyridylsulfonyl)guanyl-1-[(1,3-thiazol-2-ylamino)-carbonyl]butyl}-3-[formyl(hydroxy)amino]-2-[(4-methylcyclohexyl)-methyl]hexanamide (28g). White amorphous solid, 35%. ^{1}H NMR (400 MHz, CD_3OD, mixture of formamide rotamers and *cis/trans* 1,4-dialkylcyclohexane isomers) δ 8.57 (d, J = 4.4 Hz, 1H), 7.95 (m, 2H), 7.47 (d, J = 4.4 Hz, 1H), 7.42 (d, J = 3.2 Hz, 1H), 4.59 (m, 1H), 4.35 (m, 0.33H), 3.59 (m, 0.67H), 2.78 (m, 2H), 2.0−1.0 (m, 16H), 0.9−0.6 (m, 10H) ppm (1H not obsvd.). λ_{max} 265 nm. ESIMS *m/z* 665 $(M+H)^+$, 687 $(M+Na)^+$. Anal. ($C_{29}H_{44}N_8O_6S_2\cdot 1H_2O$) C, H, N, S.

(2*R*,3*S*)-*N*-{(1*S*)-4-(2-Pyridylsulfonyl)guanyl -1-[(1,3-thiazol-2-ylamino)carbonyl]butyl}-3-[formyl(hydroxy)-amino]-4-methyl-2-[(4-methylcyclohexyl)methyl]pentanamide (28h). White amorphous solid, 32%. ^{1}H NMR (400 MHz, CD_3OD, mixture of formamide rotamers and *cis/trans* 1,4-dialkylcyclohexane isomers) δ 8.56 (d, J = 4.8 Hz, 1H), 7.95 (m, 2H), 7.47 (m, 1H), 7.42 (m, 1H), 7.11 (m, 1H), 4.59 (m, 1H), 4.25 (m, 0.33H), 3.52 (m, 0.67H), 3.23 (m, 2H), 3.07 (m, 1H), 2.0−1.1 (m, 16H), 1.1−1.0 (m, 4H), 1.0−0.8 (m, 3H), 0.8−0.7 (m, 3H) ppm. λ_{max} 265 nm. ESIMS *m/z* 665 $(M+H)^+$, 687 $(M+Na)^+$. Anal. ($C_{29}H_{44}N_8O_6S_2\cdot 1H_2O$) C, H, N, S.

(2*R*,3*S*)-*N*-{(1*S*)-4-(2-Pyridylsulfonyl)guanyl -1-[(1,3-thiazol-2-ylamino)carbonyl]butyl}-3-[formyl(hydroxy)-amino]-2-[(5-methyl-2-thienyl)methyl]hexanamide (28i). White amorphous solid, 33%. ^{1}H NMR (400 MHz, CD_3OD, mixture of formamide rotamers) δ 8.55 (d, J = 4.8 Hz, 1H), 7.94 (m, 2H), 7.47 (m, 1H), 7.45 (m, 1H), 7.13 (m, 1H), 6.45 (d, J = 3.0 Hz, 1H), 6.17 (d, J = 3.2 Hz, 1H), 4.54 (m, 1H), 4.50 (m, 0.33H), 3.73 (m, 0.67H), 3.19 (m, 2H), 2.95 (m, 1H), 2.86 (m, 2H), 2.11 (s, 3H), 1.9−1.1 (m, 8H), 0.84 (m, 3H) ppm. λ_{max} 265 nm. ESIMS *m/z* 665 $(M+H)^+$, 687 $(M+Na)^+$. Anal. ($C_{27}H_{36}N_8O_6S_3\cdot{}^2/_3H_2O$) C, H, N, S.

(2*R*,3*S*)-*N*-{(1*S*)-4-(2-Pyridylsulfonyl)guanyl -1-[(1,3-thiazol-2-ylamino)carbonyl]butyl}-3-[formyl(hydroxy)-amino]-2-isobutylhexanamide (28j). White amorphous solid, 40%. ^{1}H NMR (400 MHz, CD_3OD, mixture of formamide rotamers) δ 8.57 (d, J = 4.8 Hz, 1H), 7.95 (s, 2H), 7.48 (m, 1H), 7.46 (d, J = 3.2 Hz, 1H), 7.10 (d, J = 3.2 Hz, 1H), 4.56 (m, 1H), 4.33 (m, 0.33H), 3.56 (m, 0.67H), 3.24 (m, 2H), 2.77 (m, 1H), 1.9−1.4 (m, 7H), 1.4−1.3 (m, 2H), 1.1−1.0 (m, 2H), 0.90 (m, 3H), 0.82 (m, 6H) ppm. λ_{max} 265 nm. ESIMS *m/z* 611 $(M+H)^+$, 633 $(M+Na)^+$. Anal. ($C_{25}H_{38}N_8O_6S_2\cdot{}^1/_2$AcOH) C, H, N, S.

(2*R*,3*S*)-*N*-{(1*S*)-4-Nitroguanyl -1-[(1,3-thiazol-2-ylamino)carbonyl]butyl}-2-(cyclohexylmethyl)-6,6,6-trifluoro-3-[formyl(hydroxy)amino]hexanamide (28k). White amorphous solid, 38%. ^{1}H NMR (400 MHz, DMSO-d_6, mixture of formamide rotamers) δ 12.17 (bs, 1H), 9.91 (0.33H), 9.60 (0.67H), 8.53 (m, 1.67H), 8.37 (s, 0.33H), 7.95 (s, 1H), 7.46 (d, J = 3.6 Hz, 1H), 7.21 (d, J = 3.6 Hz, 1H), 4.55 (s, 1H), 4.18 (m, 0.33H), 3.60 (m, 0.67H), 3.29 (m, 2H), 2.75 (m, 1H), 2.15 (m, 2H), 2.0−1.4 (m, 11H), 1.2−1.0 (m, 6H), 0.9−0.6 (m, 2H) ppm (2 Hs not obsvd). Anal. ($C_{23}H_{35}F_3N_8O_6S\cdot{}^1/_4Et_2O$) C, H, N, S.

(2*R*)-*N*-{(1*S*)-4-Nitroguanyl -1-[(1,3-thiazol-2-ylamino)-carbonyl]butyl}-2-{(1*S*)-1-[formyl(hydroxy)amino]-2-phenylethyl}-4-methylpentanamide (28l). White amorphous solid, 53%. ^{1}H NMR (400 MHz, DMSO-d_6, mixture of formamide rotamers) δ 12.21 (bs, 1H), 9.83 (s, 0.33H), 9.65 (s, 0.67H), 8.55 (d, J = 6.4 Hz, 1H), 8.5 (bs, 1H), 8.4−7.8 (bs, 2H), 7.47 (d, J = 3.2 Hz, 1H), 7.43 (s, 1H), 7.3−7.0 (m, 6H), 4.56 (m, 1H), 4.44 (m, 0.33H), 3.69 (m, 0.67H), 3.18 (m, 2H), 2.84 (m, 2H), 1.8−1.4 (m, 6H), 1.06 (m, 1H), 0.89 (d, J = 6.4 Hz, 3H), 0.77 (d, J = 6.4 Hz, 3H) ppm (1H not obsrvd.). λ_{max} 270 nm. ESIMS *m/z* 563 $(M+H)^+$. HRMS calcd for $[C_{25}H_{34}N_8O_6S]H^+$, 563.2400; found, 563.2409. Anal. ($C_{24}H_{34}N_8O_6S\cdot{}^1/_2H_2O$) C, H, N, S.

(2*R*,3*S*)-*N*-{(1*S*)-4-Methanesulfonylguanyl -1-[(1,3-thiazol-2-ylamino)carbonyl]butyl}-3-[formyl(hydroxy)amino]-2-isobutyl-4-methylpentanamide (28m). White amorphous solid, 11%. ^{1}H NMR (400 MHz, CD_3OD mixture of formamide rotamers) δ 8.33 (s, 0.33H), 7.93 (s, 0.67H), 7.41 (d, J = 3.6 Hz, 1H), 7.10 (d, J = 3.6, 1H), 4.61 (m, 1H), 4.28 (m, 0.33H), 3.46 (m, 0.67H), 3.21 (m, 0.67H), 3.00 (m, 0.33H), 2.86 (s, 3H), 2.0−1.4 (m, 7H), 1.18 (m, 1H), 1.1−1.0 (m, 3H), 0.95−0.90 (m, 6H), 0.81 (d, J = 6.4 Hz, 3H) ppm. λ_{max} 268 nm. LC R_t = 5.15 min. and 5.53 min. ESIMS *m/z* 548 $(M+H)^+$. HRMS calcd for $[C_{25}H_{34}N_8O_6S]H^+$, 548.2325; found, 548.2319.

(2*R*,3*S*)-*N*-{(1*S*)-4-Methanesulfonylguanyl -1-[(1,3-thiazol-2-ylamino)carbonyl]butyl}-3-[formyl(hydroxy)amino]-2-isobutylhexanamide (28n). White amorphous solid, 39%. ^{1}H NMR (400 MHz, DMSO-d_6, mixture of formamide rotamers) δ 9.67 (s, 0.33), 9.41 (s, 0.67H), 8.44 (m, 1H), 8.32 (s, 0.33H), 7.91 (s, 0.67H), 7.44 (d, J = 3.6 Hz, 1H), 7.18 (d, J = 3.6 Hz, 1H), 7.0−6.6 (m, 1H), 6.47 (bs, 1H), 4.48 (m, 1H), 4.13 (t, J = 10 Hz, 0.33H), 3.45 (t, J = 10 Hz, 0.67H), 3.04 (m, 2H), 2.71 (s, 3H), 2.67 (m, 1H), 1.7−0.9 (m, 11H), 0.9−0.6 (m, 9H) ppm. λ_{max} 268 nm. ESIMS *m/z* 548 $(M+H)^+$. Anal. ($C_{21}H_{37}N_7O_6S_2\cdot{}^1/_2$AcOH) C, H, N, S.

(2*R*,3*S*)-*N*-{(1*S*)-4-Methanesulfonylguanyl -1-[(1,3-thiazol-2-ylamino)carbonyl]butyl}-3-[formyl(hydroxy)amino]-4-methyl-2-[(4-methylcyclohexyl)methyl]pentanamide (28o). White amorphous solid, 48%. ^{1}H NMR (400 MHz, DMSO-d_6, mixture of formamide rotamers and *cis/trans* cyclohexane isomers) δ 9.59 and 9.58 (s, 0.33H), 9.39 and 9.35 (s, 0.67H), 8.50 (m, 1H), 8.32 and 8.29 (s, 0.33H), 7.90 (s, 0.67H), 7.44 and 7.43 (d, J = 3.6 Hz,1H), 7.20 and 7.18 (d, J = 3.6 Hz, 1H), 7.0−6.6 (bm, 2H), 6.45 (bs, 1H), 4.52 (m, 1H), 4.08 (m, 0.33H), 3.37 (m, 0.67H), 3.04 (m, 2H), 2.91 (m, 1H), 2.17 (s, 3H), 2.0−1.0 (m, 17H), 0.96 (m, 3H), 0.8−0.7 (m, 6H) ppm (1H not observed). λ_{max} 270 nm. ESIMS *m/z* 602 $(M+H)^+$. Anal. ($C_{25}H_{43}N_7O_6S_2\cdot{}^2/_3H_2O$) C, H, N, S (S calcd 10.45, found 11.08).

(2*R*,3*S*)-*N*-{(1*S*,2*R*)-4-Methanesulfonylguanyl -2-methyl-1-[(1,3-thiazol-2-ylamino)carbonyl]butyl}-3-[formyl-(hydroxy)amino]-2-isobutylhexanamide (28p). White amorphous solid, 18%. 82:18 mixture of diastereomers. ^{1}H NMR (400 MHz, CD_3OD mixture of formamide rotamers) δ 8.37 (s, 0.33H), 7.96 (s, 0.67H), 7.42 (d, J = 3.6 Hz, 1H), 7.11 (d, J = 3.6 Hz, 1H), 4.60 (m, 1H), 4.36 (m, 0.33H), 3.57 (m, 0.67H), 3.22 (m, 2H), 2.90 (m, 1H), 2.85 (s, 3H), 2.11 (m, 1H), 1.9−1.1 (m, 10H), 1.03 (d, J = 6.8 Hz, 3H), 0.9−0.8 (m, 6H), 0.8−0.7 (m, 3H) ppm. LC−ESIMS Rt = 5.17 (82%), *m/z* 562 $(M+H)^+$; 5.74 (18%), *m/z* 562 $(M+H)^+$. λ_{max} 269 nm. HRMS calcd for $[C_{22}H_{39}N_7O_6S_2]H^+$, 562.2482; found, 562.2504.

(2*R*,3*S*)-*N*-{(1*S*,2*R*)-4-Methanesulfonylguanyl -2-methyl-1-[(1,3-thiazol-2-ylamino)carbonyl]butyl}-6,6,6-trifluoro-3-[formyl(hydroxy)amino]-2-isobutylhexanamide (28q). White amorphous solid, 26%. ^{1}H NMR (400 MHz, $CDCl_3/CD_3OD$ 1:1, mixture of formamide rotamers) δ 8.38 (s, 0.33H), 7.92 (s, 0.67H), 7.40 (d, J = 3.6 Hz, 1H), 7.01 (d, J = 3.6 Hz, 1H), 4.66 (m, 1H), 4.35 (m, 0.33H), 3.62 (m, 0.67H), 3.26 (m, 2H), 2.88 (s, 3H), 2.17 (m, 1H), 2.2−1.9 (m, 4H), 1.7−1.4 (m, 5H), 1.2−1.0 (m, 1H), 0.97 (m, 3H), 0.87 (m, 3H), 0.77 (m, 3H) ppm. LC−ESIMS Rt = 5.17 (>98%), *m/z* 616 $(M+H)^+$. Anal. ($C_{22}H_{36}F_3N_7O_6S_2\cdot{}^3/_4H_2O$) C, H, N.

(2*R*,3*S*)-*N*-{(1*S*,2*R*)-4-Methanesulfonylguanyl -2-methyl-1-[(1,3-thiazol-2-ylamino)carbonyl]butyl}-3-[formyl-(hydroxy)amino]-2-isobutyl-4-methylpentanamide (28r). White amorphous solid, 17%. 85:15 mixture of diastereomers. ^{1}H NMR (400 MHz, CD_3OD mixture of formamide rotamers) δ 8.34 (s, 0.33H), 7.94 (s, 0.67H), 7.42 (d, J = 3.6 Hz, 1H), 7.10 (d, J = 3.6 Hz, 1H), 4.60 (m, 1H), 4.27 (m, 0.33H), 3.53 (m, 0.67H), 3.25 (m, 2H), 3.1−3.0 (m, 1H), 2.85 (s, 3H), 2.11 (m, 1H), 1.92 (m, 1H), 1.62 (m, 1H), 1.5−1.3 (m, 3H), 1.1 (m, 3H), 1.0 (m, 3H), 0.9 (m, 6H), 0.77 (d, J = 6.8 Hz, 3H) ppm.

LC−ESIMS Rt = 4.98 (85%), *m/z* 562 $(M+H)^+$; 5.38 (15%), *m/z* 562 $(M+H)^+$. λ_{max} 270 nm. Anal. ($C_{22}H_{39}N_7O_6S_2 \cdot {}^3/_4H_2O$) C, H, N.

(2*R*,3*S*)-*N*-{(1*S*,2*R*)-4-Nitroguanyl-2-methyl-1-[(1,3-thiazol-2-ylamino)carbonyl]butyl}-3-[formyl(hydroxy)amino]-2-isobutylhexanamide (28s). White amorphous solid, 35%. 90:10 mixture of diastereomers. ^{1}H NMR major diastereomer (400 MHz, CD_3OD mixture of formamide rotamers) δ 8.37 (s, 0.33H), 7.97 (s, 0.67H), 7.42 (d, J = 3.6 Hz, 1H), 7.11 (d, J = 3.6 Hz, 1H), 4.65 (m, 1H), 4.36 (m, 0.33H), 3.61 (0.67H), 3.36 (m, 2H), 2.92 (m, 0.67H), 2.84 (m, 0.33H), 2.15 (m, 1H), 1.8−1.1 (m, 8H), 1.03 (d, J = 6.8 Hz, 3H), 0.95 (m, 1H), 0.91 (m, 6H), 0.78 (m, 3H) ppm. LC−ESIMS Rt = 5.25 (90%), *m/z* 529 $(M+H)^+$; 5.84 (10%), *m/z* 529 $(M+H)^+$. λ_{max} 270 nm. Anal. ($C_{21}H_{36}N_8O_6S \cdot {}^3/_4H_2O$) C, H, N.

(2*S*,3*R*)-5-Nitroguanyl -2-[((2*R*)-2-{(1*S*)-1-[formyl(hydroxy)amino]ethyl}-4-methylpentanoyl)amino]-3-methyl-*N*-(1,3-thiazol-2-yl)pentanamide (28t). White amorphous solid, 43%. ^{1}H NMR (400 MHz, CD_3OD mixture of formamide rotamers) δ 8.28 (s, 0.33H), 7.99 (s, 0.67H), 7.42 (d, J = 3.6 Hz, 1H), 7.11 (d, J = 3.6 Hz, 1H), 4.68 (m, 1H), 4.46 (m, 0.33H), 3.81 (m, 0.67H), 3.35 (m, 2H), 2.91 (m, 0.67H), 2.88 (m, 0.33H), 2.15 (m, 1H), 1.69 (m, 1H), 1.6−1.3 (m, 3H), 1.28 (d, J = 6.8 Hz, 2H), 1.20 (d, J = 6.8 Hz, 1H), 1.1−1.0 (m, 1H), 1.02 (d, J = 6.8 Hz, 3H), 0.90 (m, 3H), 0.78 (m, 3H) ppm. LC−ESIMS Rt = 4.82 (97%) *m/z* 501 $(M+H)^+$. λ_{max} 270 nm. Anal. ($C_{19}H_{32}N_8O_6S \cdot {}^3/_4H_2O$) C, H, N.

(2*S*,3*R*)-5-Methanesulfonylguanyl -2-[((2*R*)-2-{(1*S*)-1-[formyl(hydroxy)amino]ethyl}-4-methylpentanoyl)amino]-3-methyl-*N*-(1,3-thiazol-2-yl)pentanamide (28u). White amorphous solid, 14%. ^{1}H NMR (400 MHz, CD_3OD mixture of formamide rotamers) δ 8.28 (s, 0.33H), 7.99 (s, 0.67H), 7.42 (d, J = 3.6 Hz, 1H), 7.10 (d, J = 3.6 Hz, 1H), 4.62 (m, 1H), 4,45 (m, 0.33H), 3.81 (m, 0.67H), 3.25 (m, 2H), 2.88 (m, 1H), 2.85 (s, 3H), 2.12 (m, 1H), 1.64 (m, 1H), 1.42 (m, 3H), 1.28 (d, J = 6.8 Hz, 2H), 1.18 (d, J = 6.8 Hz, 1H), 1.1−1.0 (m, 1H), 1.02 (m, 3H), 0.90 (m, 3H), 0.78 (m, 3H) ppm. LC−ESIMS Rt = 4.62 (95%) *m/z* 534 $(M+H)^+$. λ_{max} 270 nm. Anal. ($C_{20}H_{35}N_7O_6S_2 \cdot {}^2/_3CH_2Cl_2$) C, H, N.

Acknowledgment. We gratefully acknowledge Angela Hassman and Theresa Seaton for TACE assay development and Robert Johnson and Manon Villeneuve for analytical support.

Supporting Information Available: Experimental procedures and spectral characterization are provided for compounds **5a**−**t**, **6j**−**t**, and **7j**−**t**. The synthesis of β,β-dimethyl ornithine derivatives from acid **16b** and attempted conversion to β,β-dimethyl-Arg derivatives is also provided. This material is available free of charge via the Internet at http://pubs.acs.org.

References

(1) Vassalli, P. The Pathophysiology of Tumor Necrosis Factors. *Annu. Rev. Immunol.* **1992**, *10*, 411.
(2) Szatmary, Z. Tumor Necrosis Factor-α: Molecular-Biological Aspects. Minireview. *Neoplasma* **1999**, *46* (5), 257−66.
(3) Kitano, K.; Rivas, C. I.; Baldwin, G. C.; Vera, J. C.; Golde, D. W. Tumor Necrosis Factor-Dependent Production of Human Immunodeficiency Virus 1 in Chronically Infected HL-60 Cells. *Blood* **1993**, *82*, 2742−8.
(4) Elliott, M. J.; Maini, R. N.; Feldmann, M.; Kalden, J. R.; Antoni, C.; Smolen, J. S.; Leeb, B.; Breedveld, F. C.; Macfarlane, J. D.; Bijl, H. Randomised Double-Blind Comparison of Chimeric Monoclonal Antibody to Tumor Necrosis Factor Alpha (Ca2) Versus Placebo in Rheumatoid Arthritis. *Lancet* **1994**, *344*, 1105−10.
(5) Dinarello C. A. The Proinflammatory Cytokines Interleukin-1 and Tumor Necrosis Factor and Treatment of the Septic Shock Syndrome. *J. Infect. Dis.* **1991**, *163* (6), 1177−84.
(6) Hotamisligil, G. S.; Spiegelman, B. M**.** Tumor Necrosis Factor α: A Key Component of the Obesity-Diabetes Link. *Diabetes* **1994**, *43*, 1271−8.
(7) Piguet, P. F.; Grau, G. E.; Allet, B.; Vassalli, P. Tumor Necrosis Factor/Cachectin is an Effector of Skin and Gut Lesions of the Acute Phase of Graft-Vs.-Host Disease. *J. Exp. Med.* **1987**, *166*, 1280−9.
(8) Becherer, J. D.; Lambert, M. H.; Andrews, R. C. The Tumor Necrosis Factor-α Converting Enzyme. *Handb. Exp. Pharmacol.* **2000**, *140*, 235−58.
(9) Moss, M. L.; White, J. M.; Lambert, M. H.; Andrews, R. C. TACE and Other ADAM Proteases as Targets for Drug Discovery. *Drug Discovery Today* **2001**, *6* (8), 417−26.
(10) Banner, D. W.; D'Arcy, A., J.; Gentz, R. W.; Schoenfeld, H.-J.; Broger, C.; Loetscher, H.; Lesslauer, W. Crystal Structure of the Soluble Human 55 Kd TNF Receptor-Human TNFβ Complex: Implications For TNF Receptor Activation. *Cell* **1993**, *73*, 431−45.
(11) Vandenabeele, P.; Declercq, W.; Beyaert, R.; Fiers, W. Two Tumor Necrosis Factor Receptors: Structure and Function. *Trends Cell. Biochem.* **1995**, *5*, 392−9.
(12) Pfeffer, K.; Matsuyama, T.; Kundig, T. M.; Wakeham, A.; Kishihara, K.; Shahinian, A.; Wiegmann, K.; Ohashi, P. S.; Kronke, M.; Mak, T. W. Mice Deficient for the 55 Kd Tumor Necrosis Factor Receptor are Resistant to Endotoxic Shock, Yet Succumb to *L. monocytogenes* Infection. *Cell* **1993**, *73*, 457−67.
(13) Selinsky, C. L.; Boroughs, K. L.; Halsey, W. A.; Howell, M. D. Multifaceted Inhibition of Anti-Tumour Immune Mechanisms by Soluble Tumour Necrosis Factor Receptor Type I. *Immunology* **1998**, *94*, 88−93.
(14) Natarajan, K.; Manna, S. K.; Chaturvedi, M. M.; Aggarwal, B. B. Protein Tyrosine Kinase Inhibitors Block Tumor Necrosis Factor-Induced Activation of Nuclear Factor-KB, Degradation of IKBα, Nuclear Translocation of P65, and Subsequent Gene Expression. *Arch. Biochem. Biophys.* **1998**, *352*, 59−70.
(15) Khaled, A. R.; Butfiloski, E. J.; Sobel, E. S.; Schiffenbauer, J. Use of Phosphorothioate-Modified Oligodeoxynucleotides to Inhibit NF-κB Expression and Lymphocyte Function. *Clin. Immunol. Immunopathol.* **1998**, *86*, 170−9.
(16) Aggarwal, B. B.; Schwarz, L.; Hogan, M. E.; Rando, R. F. Triple Helix-Forming Oligodeoxyribonucleotides Targeted to the Human Tumor Necrosis Factor (TNF) Gene Inhibit TNF Production and Block the TNF-Dependent Growth of Human Glioblastoma Tumor Cells. *Cancer Res.* **1996**, *56*, 5156−64.
(17) Onrust, S. V.; Lamb, H. M. Infliximab: A Review of its Use in Crohn's Disease and Rheumatoid Arthritis. *BioDrugs* **1998**, *10* (5), 397−422.
(18) Murray, K. M.; Dahl, S. L. Recombinant Human Tumor Necrosis Factor Receptor (P75) Fc Fusion Protein (TNFR:Fc) in Rheumatoid Arthritis. *Ann. Pharmacother.* **1997**, *31*, 1335−8.
(19) Hamilton, K.; Clair, E. W. Tumour Necrosis Factor-Alpha Blockade: A New Era for Effective Management of Rheumatoid Arthritis. *Expert Opin. Pharmacother.* **2000**, *1* (5), 1041−52.
(20) Hanauer, S. B. Safety of Infliximab in Clinical Trials. *Aliment. Pharmacol. Ther.* **1999**, *13* (Suppl. 4), 16−22.
(21) Watts, R. A. Musculoskeletal and Systemic Reactions to Biological Therapeutic Agents. *Curr. Opin. Rheumatol.* **2000**, *12* (1), 49−52.
(22) Murali, R.; Hasegawa, A.; Berezov, A.; Kajino, K.; Takasaki, W. Design and Development of Small-Molecule Inhibitor of Tumor Necrosis Factor-α. In *Cytokine Inhibitors*; Ciliberto, G., Savino, R., Eds.; Marcel Dekker: New York, 2001; pp 133−61.
(23) Gum, R. J.; Young, P. R. p38 Inhibition. In ref 22, pp 329−61.
(24) Gearing, A. J. H.; Beckett, P.; Christodoulou, M.; Churchill, M.; Clements, J.; Davidson, A. H.; Drummond, A. H.; Galloway, W. A.; Gilbert, R.; Gordon, J. L.; Leber, T. M.; Mangan, M.; Miller, K.; Nayee, P.; Owen, K.; Patel, S.; Thomas, W.; Wells, G.; Wood, L. M.; Wolley, K. Processing of Tumour Necrosis Factor-α Precursor by Metalloproteinases. *Nature* **1994**, *370*, 555−7.
(25) Mohler, K. M.; Sleath, P. R.; Fitzner, J. N.; Cerretti, D. P.; Alderson, M.; Kerwar, S. S.; Dauphine S. T.; Otten-Evans, C.; Greenstreet, T.; Weerawarna, K.; Kronheim, S. R.; Petersen, M.; Gerhart, M. Kozlosky, M.; March, C. J.; Black, R. A. Protection Against a Lethal Dose of Endotoxin by an Inhibitor of Tumour Necrosis Factor Processing. *Nature* **1994**, *370*, 218−20.
(26) McGeehan, G. M.; Becherer, J. D.; Bast, R. C., Jr.; Boyer, C. M.; Champion, B.; Connolly, K. M.; Conway, J. G.; Furdon, P.; Karp, S.; Kidao, S.; McElroy, A. B.; Nichols, J.; Pryzwansky, K. M.; Schoenen, F.; Sekut, L.; Truesdale, A.; Verghese, M.; Warner, J.; Ways, J. P. Regulation of Tumour Necrosis Factor-α Processing by a Metalloproteinase Inhibitor. *Nature* **1994**, *370*, 558−61.
(27) Black, R. A.; Rauch, C. T.; Kozlosky, C. J.; Peschon, J. J.; Slack, J. L.; Wolfson, M. F.; Castner, B. J.; Stocking, K. L.; Reddy, P.; Srinivasan, S.; Nelson, N.; Boiani, N.; Schooley, K. A.; Gerhart, M.; Davis, R.; Fitzner, J. N.; Johnson, R. S.; Paxton, R. J.; March, C. J.; Cerretti, D. P. A Metalloproteinase Disintegrin that Releases Tumor-Necrosis Factor-α from Cells. *Nature* **1997**, *385*, 729−33.
(28) Moss, M. L.; Jin, S.-L. C.; Milla, M. E.; Bickett, D. M.; Burkhart, W.; Carter, H. L.; Chen, W.-J.; Clay, W. C.; Didsbury, J. R.; Hassler, D.; Hoffman, C. R.; Kost, T. A.; Lambert, M. H.; Leesnitzer, M. A.; McCauley, P.; McGeehan, G.; Mitchell, J.;

Moyer, M.; Pahel, G.; Rocque, W.; Overton, L. K.; Schoenen, F.; Seaton, T.; Su, J.-L.; Warner, J.; Willard, D.; Becherer, J. D. Cloning of a Disintegrin Metalloproteinase That Processes Precursor Tumor-Necrosis Factor-α. *Nature* **1997**, *385*, 733−6.
(29) Black, R. A.; White, J. M. ADAMS: Focus on the Protease Domain. *Curr. Opin. Cell Biol.* **1998**, *10*, 654−9.
(30) Schlondorff, J.; Becherer, J. D.; Blobel, C. P. Intracellular Maturation and Localization of the Tumour Necrosis Factor α Convertase (TACE). *Biochem. J.* **2000**, *347* (1), 131−8.
(31) Moss, M. L.; Becherer, J. D.; Conway, J. G.; Warner, J. R.; Bickett, D. M.; Leesnitzer, M. A.; Seaton, T. M.; Mitchell, J. L.; McConnell, R. T.; Tippin, T. K.; Whitesell, L. G.; Rizzolio, M. C.; Hedeen, K. M.; Beaudet, E. J.; Andersen, M.; Lambert, M. H.; Austin, R.; Stanford, J. B.; Bubacz, D. G.; Chan, J. H.; Schaller, L. T.; Gaul, M. D.; Cowan, D. J.; Boncek, V. M.; Rabinowitz, M. H.; Musso, D. L.; McDougald, D. L.; Kaldor, I.; Glennon, K.; Wiethe, R. W.; Guo, Y.; Andrews, R. C**.** Screening and Design of Tumor Necrosis Factor-α: Converting Enzyme Inhibitors; in ref 22; pp 163−76.
(32) Voss, M. E.; Decicco, C. P.; Wexler, R. R. Preparation of Arylsulfonylheterocyclylhydroxamic Acids as Metalloproteinase and TNF Inhibitors for the Treatment of Inflammatory Disorders. PCT Int. Appl. 1999, WO 9958531 A1 19991118.
(33) Bird, J.; Montana, J. G.; Wills, R. E.; Baxter, A. D.; Owen, D. A. Selective Matrix Metalloproteinase (MMP) Inhibitors Having Reduced Side-Effects. PCT Int. Appl. 1998, WO 9839024 A1 19980911.
(34) Becherer, J. D. TACE: A Disintegrin Metalloprotease that Regulates TNF-α Production *In vitro* and *In vivo*, New York Academy of Sciences Conference on Inhibition of Matrix Metalloproteinases: Therapeutic Applications, Tampa, FL, Oct. 1998.
(35) Conway, J. G.; Andrews, R. C.; Beaudet, B.; Bickett, D. M.; Boncek, V.; Brodie, T. A.; Clark, R. L.; Crumrine, R. C.; Leenitzer, M. A.; McDougald, D. L.; Han, B.; Hedeen, K.; Lin, P.; Milla, M.; Moss, M.; Pink, H.; Rabinowitz, M. H.; Tippin, T.; Scates, P. W.; Selph, J.; Stimpson, S. A.; Warner, J.; Becherer, J. D. Inhibition of tumor necrosis factor-α (TNF-α) Production and Arthritis in the Rat by GW3333, a Dual Inhibitor of TNF-α Converting Enzyme and Matrix Metalloproteinases. *J. Pharmacol. Exp. Ther.* **2001**, *298* (3), 900−8.
(36) Andrews, R. C.; Anderson, M. W.; Stanford, J. B.; Bubacz, D. G.; Chan, J. H.; Cowan, D. J.; Gaul, M. D.; McDougald, D. L.; Musso, D. L.; Rabinowitz, M. H.; Wiethe, R. W. Preparation of *N*-Formyl-*N*-Hydroxypeptide Analogues as Metalloprotease Inhibitors. Brit. UK Pat. Appl. GB 2348198 A1, 2000.
(37) Lambert, M. H., unpublished results.
(38) Gomis-Ruth, F. X.; Kress, L. F.; Kellermann, J.; Mayr, I.; Lee, X.; Huber, R.; Bode, W. Refined 2.0 Å X-ray Crystal Structure of the Snake Venom Zinc Endopeptidase Adamalysin II. Primary and Tertiary Structure Determination, Refinement, Molecular Structure and Comparison with Astacin, Collagenase and Thermolysin. *J. Mol. Biol.* **1994**, *239*, 513−44.
(39) Lambert, M. H. Docking Conformationally Flexible Molecules Into Protein Binding Sites. In *Practical Application of Computer-Aided Drug Design*; Charifson, P. S., Ed.; Marcel Dekker: New York, 1997; pp 243−303.
(40) The pK_a of the nitroguanidinium ion in water was measured to be −0.98. Taylor, P. J.; Wait, A. R. σ_1 Values for Heterocycles. *J. Chem. Soc., Perkin Trans. 2*, **1986**, 1765−70.
(41) Maskos, K.; Fernandez-Catalan, C.; Huber, R.; Bourenkov, G. P.; Bartunik, H.; Ellestad, G. A.; Reddy, P.; Wolfson, M. F.; Rauch, C. T.; Castner, B. J.; Davis, R.; Clarke, H. R. G.; Petersen, M.; Fitzner, J. N.; Cerretti, D. P.; March, C. J.; Paxton, R. J.; Black, R. A.; Bode, W. Crystal Structure of the Catalytic Domain of Human Tumor Necrosis Factor-α-Converting Enzyme. *Proc. Natl. Acad. Sci. U.S.A.* **1998**, *95* (7), 3408−12.
(42) Bickett, D. M.; Green, M. D.; Berman, J.; Dezube, M.; Howe, A. S.; Brown, P. J.; Roth, J. T.; McGeehan, G. M. A High Throughput Fluorogenic Substrate for Interstitial Collagenase (MMP-1) and Gelatinase (MMP-9). *Anal. Biochem.* **1993**, *212*, 58−64.
(43) Leesnitzer, M. A.; Bickett, D. M.; Moss, M. L.; Becherer, J. D. A High Throughput Assay for the TNF Converting Enzyme. *High Throughput Screening for Novel Anti-inflammatories*. Birkhauser Verlag: Basel, Switzerland, 2000; pp 87−100.
(44) Ziegler-Heitbrook, H. W. L.; Thiel, E.; Fuetter, A.; Herzog, V.; Wirtz, A.; Reithmueller, G. Establishment of a Human Cell Line (Mono Mac 6) with Characteristics of Mature Monocytes. *Int. J. Cancer* **1988**, *41*, 456−61.
(45) Noyori, R.; Ohkuma, T.; Kitamura, M.; Takaya, H.; Sayo, N.; Kumobayashi, H.; Akutagawa, S. Asymmetric Hydrogenation of *β*-Keto Carboxylic Esters. A Practical, Purely Chemical Access to *β*-Hydroxy Esters in High Enantiomeric Purity. *J. Am. Chem. Soc.* **1987**, *109* (19), 5856−8.
(46) Seebach, D.; Aebi, J.; Wasmuth, D. Diastereoselective α-Alkylation of *β*-Hydroxycarboxylic Esters Through Alkoxide Enolates: (+)-Diethyl (2S, 3R)-3-Allyl-2-Hydroxysuccinate from (−)-Diethyl S-Malate (Butanedioic Acid, 2-Hydroxy-3-(2-Propenyl)-, Diethyl Ester, [S−(R, S)]). *Org. Synth.* **1985**, *63*, 109−20.
(47) Krimen, L. I. Acetic Formic Anhydride. *Org. Synth.* **1970**, *50*, 1−3.
(48) Hanessian, S.; Kagotani, M.; Komaglou, K. Design and Reactivity of Organic Functional Groups − 2-Pyridylsulfonates as Nucleofugal Esters: Remarkably Mild Transformations into Halides and Olefins. *Heterocycles* **1989**, *28* (2), 1115−20.
(49) Kazmaier, U.; Krebs, A. Synthesis of Chiral *γ*,*δ*-Unsaturated Amino Acids by Asymmetric Ester Enolate Claisen Rearrangement. *Angew. Chem., Int. Ed. Engl.* **1995**, *34* (18), 2012−4.
(50) Krebs, A.; Kazmaier, U. The Asymmetric Ester Enolate Claisen Rearrangement as a Suitable Method for the Synthesis of Sterically Highly Demanding Amino Acids. *Tetrahedron Lett.* **1996**, *37* (44), 7945−6.
(51) Allinger, N. L.; Zalkow, V. Conformational Analysis. IX. gem-Dimethyl Effect. *J. Org. Chem.* **1960**, *25*, 701−4.
(52) Avontuur, J. A. M.; Buijk, S. L. C. E.; Bruining, H. A. Distribution and Metabolism of N^G-Nitro-L-Arginine Methyl Ester in Patients with Septic Shock. *Eur. J. Clin. Pharmacol.* **1998**, *54* (8), 627−31.
(53) Henke, B. R.; Blanchard, S. G.; Brackeen, M. F.; Brown, K. K.; Cobb, J. E.; Collins, J. L.; Harrington, W. W., Jr.; Hashim, M. A.; Hull-Ryde, E. A.; Kaldor, I.; Kliewer, S. A.; Lake, D. H.; Leesnitzer, L. M.; Lehmann, J. M.; Lenhard, J. M.; Orband-Miller, L. A.; Miller, J. F.; Mook, R. A.; Noble, S. A.; Oliver, W.; Parks, D. J.; Plunket, K. D.; Szewczyk, J. R.; Willson, T. M. N-(2-Benzoylphenyl)-L-tyrosine PPARγ Agonists. 1. Discovery of a Novel Series of Potent Antihyperglycemic and Antihyperlipidemic Agents. *J. Med. Chem.* **1998**, *41* (25), 5020−36.

JM0102654